

REVIEW ARTICLE

CONE BEAM CT: NON-DENTAL APPLICATIONS

J.W. Casselman^{1,3,4}, K. Gieraerts¹, D. Volders¹, J. Delanote¹, K. Mermuys¹, B. De Foer³, G. Swennen²

Initially Cone Beam CT was almost exclusively used to perform dental radiology. However, the first generation CBCT systems were later increasingly used to study sinuses, facial and nose fractures, temporomandibular joints etc. 3D-cephalometric head and neck studies became possible once CBCT systems were available that allowed scanning of the complete head. For this purpose a double rotation technique with stitching of the resulting two data sets was needed. CBCT systems on which the rotation could be stopped were needed to perform dynamic swallow or pharyngography studies. The advent of more powerful high-end CBCT systems led the way to temporal bone and skull base imaging. Finally, high-end “supine” CBCT systems using a “gantry” made small joint musculoskeletal imaging possible. These non-dental CBCT studies gradually replaced conventional X-rays and CT/MDCT studies because they allowed imaging with higher resolution, lower radiation dose and less metal artifacts. In this paper the most important non-dental CBCT indications will be discussed.

Key-words: Computed tomography (CT), cone beam – Temporal bone, CT – Paranasal sinuses, CT.

Initially, Cone Beam CT was almost exclusively used to perform dental radiology. The first major application was presurgical planning of implant placement (1). In these patients cross-sectional imaging provided additional information and especially avoided damage to the inferior alveolar nerve during implantation. The second major indication was the evaluation of the relation between impacted wisdom teeth and the inferior alveolar canal prior to extraction. Many other applications followed: tooth impaction, supplementary and supernumerary teeth, tooth agenesis, cleft lip and palate, preoperative evaluation in maxillofacial surgery, dental- jaw trauma, cysts and benign lesions of the jaws, and finally also orthodontic and endodontic problems (2). Before 3D introduction, dental plain films and panoramic radiographs were mostly used for the above indications. However, conventional CT and multidetector CT (MDCT) gradually replaced these imaging modalities. The major drawbacks of these conventional CT systems were the moderate spatial resolution of 500 micrometer (μm) or higher and the higher radiation burden which withheld the clinicians to ask for CT studies especially in younger patients. The advent of Cone Beam CT systems using 10-100 microsievert (μSv) and resolutions down to 200 μm took away most restraints. This was not always justified as some of the early Cone

Table I. – Most frequent dental indications (based on 899 CBCT studies performed during 2 consecutive months in 2012).

Presurgical implant planning	64%
Endodontics – periodontology	19,5%
Pre-operative screening (cardiac surgery etc.)	10%
Pre-operative wisdom teeth removal	4,5%
Trauma	2%

Beam CT systems used an effective radiation dose of up to 1200 μSv which is an equivalent of 240 panoramic radiographs (3). Nevertheless newer CBCT systems in general use a lower radiation dose than conventional CT's (4-6) and reach a spatial resolution of 100 μm or less. This latter characteristic gave CBCT the status of a valuable “endodontic” diagnostic technique. It was obvious that the strongest trumps of CBCT, lower radiation dose, higher spatial resolution and less metal artifacts also applied in other head and neck regions (7). The major drawback remains the long acquisition time of 10 to 40 seconds. It is not possible to perfectly immobilize young children and less cooperative especially edentulous elderly people for such a long time and therefore these patients are better studied with fast MDCT. Extensive literature on the CBCT technique and dental CBCT indications (Table I), today accounting for 27% of the studies in our hospital (Table II), is already available (8). Be-

low the most established and new non-dental applications will be discussed.

CBCT 3D-cephalometric analysis

Conventional lateral cephalograms were used for many years for orthodontic assessment, treatment and follow-up. On these 2D projection images both the bony structures and the overlying soft tissues could be evaluated and measured prior to surgery or non-surgical orthodontic treatment. Maxillofacial surgeons however dreamed of 3D-data which would allow them to make 3D-cephalograms and to achieve more exact presurgical assessment and planning (Fig. 1). This became possible on conventional CT and MDCT but the much higher radiation dose and low spatial resolution hampered further use of this technique at that stage. These inconveniences were overcome with CBCT. CBCT 3D-cephalography became the second major CBCT application as dentists and maxillofacial surgeons were the first to have access to CBCT (9, 10). This was however not possible before a major technical problem was tackled: the small size of the flat panel detectors. Most CBCT detectors have

From: Department of 1. Radiology and Medical Imaging and 2. Maxillo-Facial Surgery, AZ St. Jan Brugge AV, Brugge, Belgium, 3. Department of Radiology, AZ St. Augustinus, Wilrijk, Belgium, 4. University of Gent, Gent, Belgium.
Address for correspondence: Pr J.W. Casselman, M.D., Ph.D., Department of Radiology, AZ St. Jan Brugge AV, Ruddershove 10, 8000 Brugge, Belgium.

Table II. — Most frequent cone beam CT indications (based on 899 CBCT studies performed during 2 consecutive months in 2012).

Sinus	38%
Dental	26,5%
MSK	14%
3D-Cephalogram	10%
Maxillofacial	5%
Temporal bone	4,5%
Vertex	1%
TMJ	0,5%
Miscellaneous	0,5%

a height of 13 cm and a width of 23 cm and therefore it is impossible to image the facial structures from the upper larynx to the forehead and to include both external auditory canals as well. To achieve this the "double rotation" technique was introduced. A first CBCT acquisition (full rotation) centered on the lower half of the facial structures is followed by a second CBCT acquisition centered on the upper half of the facial structures. A considerable overlap is used to avoid artifacts at the interface and a final "extended field-of-view (FOV)" image of 17 cm high x 23 cm wide can be achieved by software "stitching" of the two 13 x 23 cm data sets (Fig. 1a). Patient immobilization is crucial as the X-ray

tube and flat panel detector must be displaced during this double rotation acquisition. Another solution uses vertical rotation of the flat panel detector. This solves the problem of the image height but reduces the image size in the transverse plane making it often difficult to include the nasion and both external auditory canals and overlying soft tissues. Initially these images were predominantly used in young patients for pre-surgical assessment, planning and follow-up of patients requiring orthodontic (11) (Fig. 2), cleft lip and palate (12, 13) and major congenital facial malformation/deformity corrective surgery (Fig. 3). In these young patients repetitive imaging is often needed and therefore CBCT's using a low ra-

diation dose are preferred. Another requirement is that these patients must be scanned in the sitting position in order to evaluate the soft tissues in their natural upright position and therefore CBCT's with a trolley designed to scan patients in the supine position can't be used for this application. It also became gradually possible to superimpose 3D laser acquired data of the soft tissues of the face on top of the bony skull image generated by the CBCT. This was at first only possible with the development and use of dedicated "image-matching" software (Fig. 2). Fully integrated facial scanning only became possible with newer CBCT systems that enable concomitant 3D laser acquisition of the soft tissues of the face during the CBCT acquisition (1), potentially providing more accurate 3D information as both data sets are acquired at the same time with the patient immobilized in the same position. The same CBCT technique can of course also be applied in other patients like those requiring jaw bone or facial bone reconstruction following destruction by a malignant tumor (Fig. 4) etc. Today 3D-cephalometric CBCT studies are the fourth most frequent CBCT indication and account for 10% of all CBCT studies in our department although this is probably somewhat biased by the

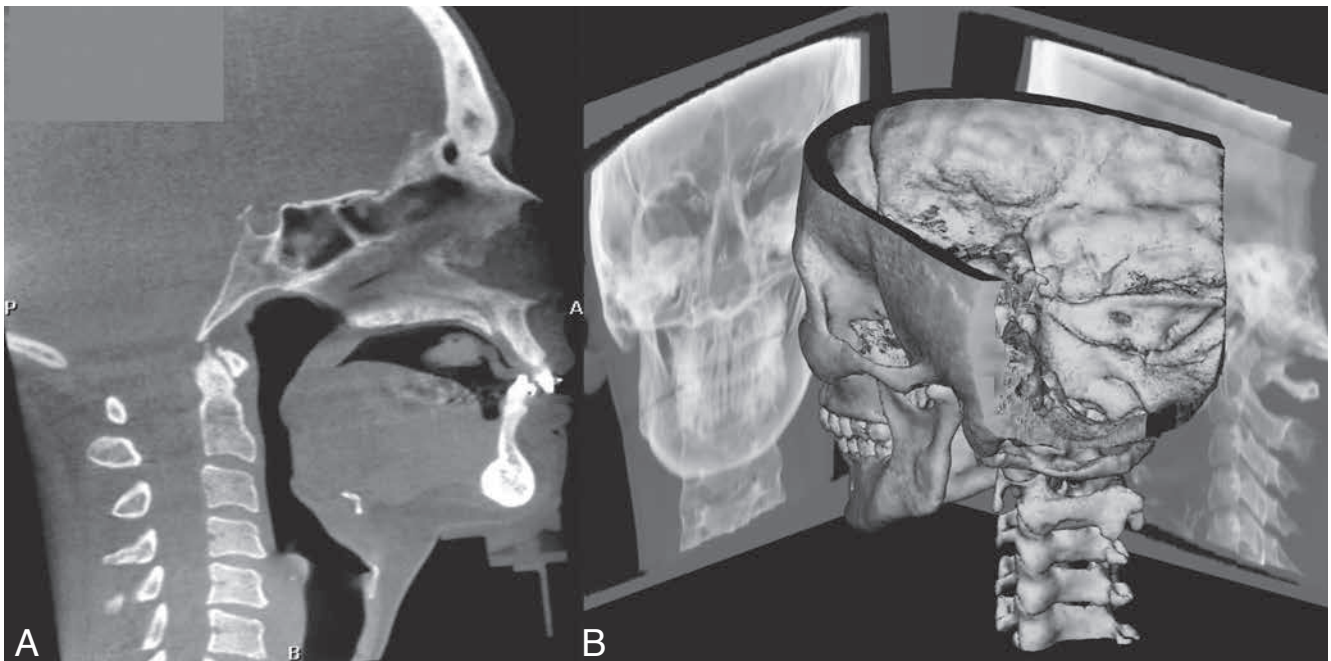


Fig. 1. — Extended field of view (FOV) CBCT acquired with the double rotation technique covering all the necessary structures from the larynx to the forehead.

Stitched extended FOV CBCT image, one of the 360 (lateral) views used to reconstruct the 3D CBCT images (A). These 3D CBCT images can provide more accurate measurements than the 2D projection conventional cephalograms. Both the 3D CBCT images and 2D projections (cephalograms) made from these 3D CBCT images can be made from the CBCT data set (B).

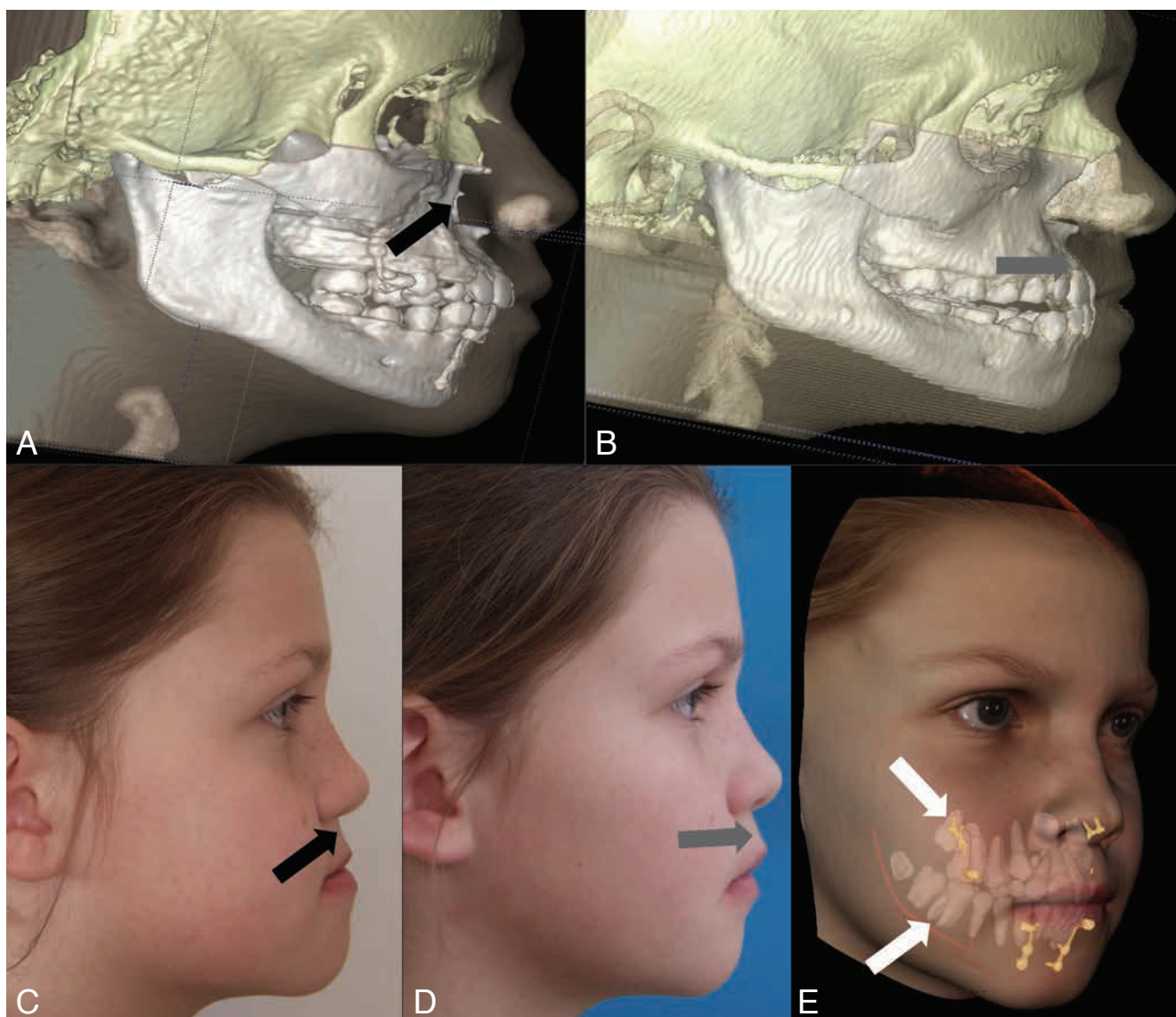


Fig. 2. — Three-dimensional analysis of maxillary protraction with intermaxillary elastics to miniplates. A,B: Three-dimensional CBCT reconstruction of the face pre-treatment (A) and after protraction (B) showing the retrognathia (black arrow) and correction after treatment (grey arrow). C,D: Clinical image of pre-treatment maxillary retrognathia (C) (black arrow) and correction after protraction (D) (grey arrow). E: Superimposed 3D laser acquired data on the CBCT acquired 3D reconstruction of the teeth (white arrows).

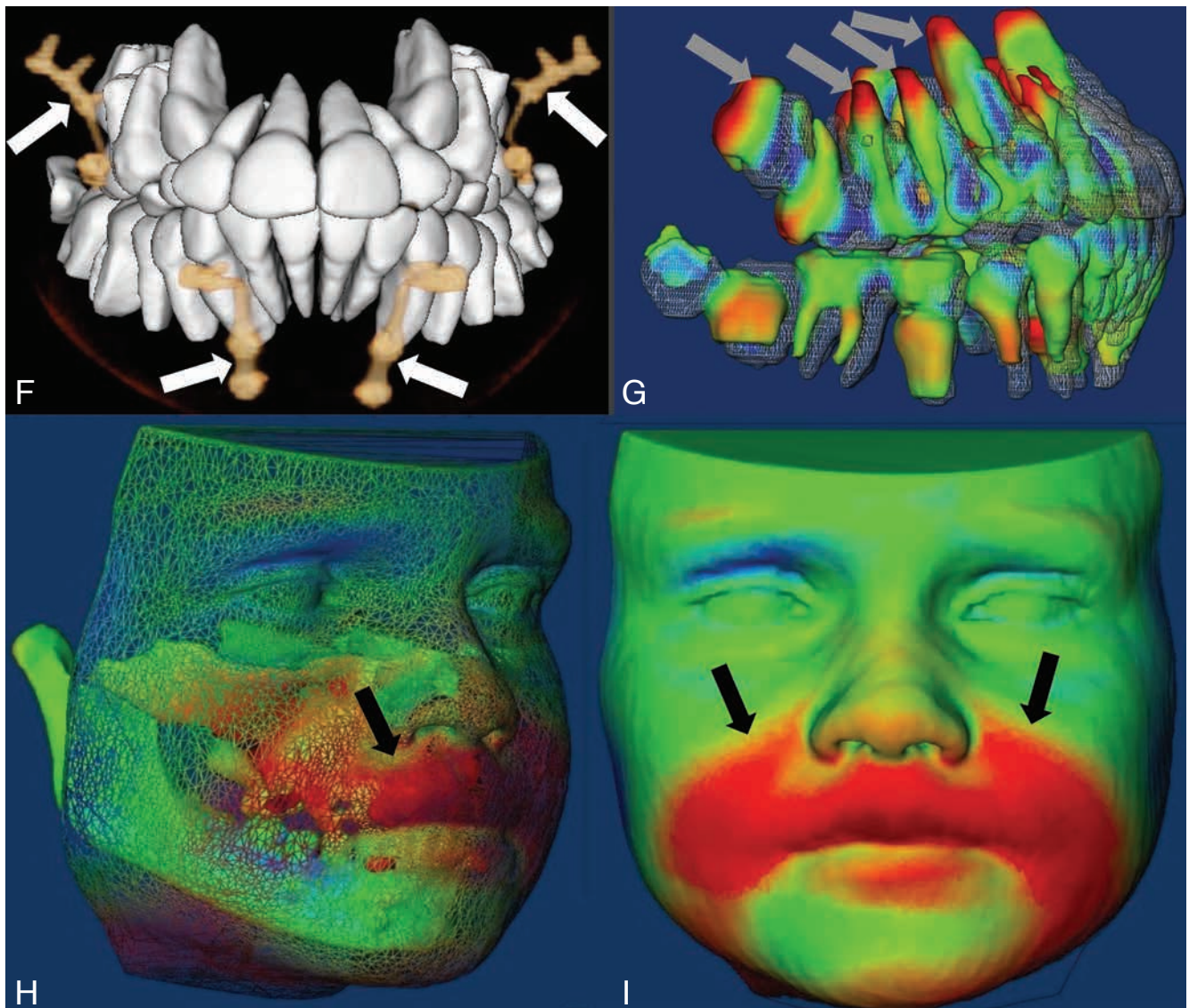
specific high referral pattern of these patients in our hospital (Table I).

CBCT of the sinuses

The first real CBCT application outside the dental and maxilla-facial field was sinus imaging. Several years ago low dose MDCT of the sinuses replaced the conventional X-rays of the sinuses and became the golden standard and it took a couple years again before it was challenged by CBCT. Nevertheless the first experiences were dental again and concerned odontogenic sinusitis and evaluation of the osteomeatal unit

(OMU) in oral implant candidates (14-16). Many studies demonstrated that similar low dose scanning can be achieved with MDCT and CBCT. Low dose imaging is crucial as inflammatory sinus disease is often recurring and results in repetitive imaging requests. However, at such a low dose MDCT images become very "noisy", are degraded by metal artifacts and still have a moderate spatial resolution in comparison with CBCT. Hence, although the radiation dose can be similar the MDCT image quality is no longer comparable with the quality provided by good and/or high-end CBCT's. It is also important

to know that the use of a small FOV is one of the easiest ways to further reduce the radiation dose. Good collimation and planning allows imaging of the sinuses using a 8 cm (h) x 8cm (d) FOV instead of a 12 cm (h) x 12 cm (d) FOV which results in a 70% dose reduction. A major advantage of CBCT is that images have the same quality in all possible planes. This allows the ENT surgeon to evaluate the OMU and frontal sinus drainage anatomy in detail prior to acute or chronic sinusitis surgery (Fig. 5, 6). For this indication CBCT with the lowest possible radiation dose can be used and provides all



F: Post-treatment AP image with only visualization of the teeth and the bone anchored miniplates (white arrows). G: Lateral view with superimposed pre- and post-treatment CBCT image of the teeth. Red color indicates displacement upper teeth by the treatment (grey arrows), green indicates that the structures were not displaced during the treatment. H,I: Superimposed pre- and post-treatment 3D CBCT soft tissue surface reconstructions showing that the treatment selectively corrected the retrognathia and overlying soft tissues (red color)(black arrows) while the other structures remained uninvolved (green color). Follow-up studies in young patients can only be justified when the radiation is very low and this became possible with the advent of CBCT.

Courtesy: Prof. De Clerck H, St-Luc Hospital, UCL, Brussels, Belgium and Prof. Lucia Cevidanes, Chapel Hill, North Carolina, USA.

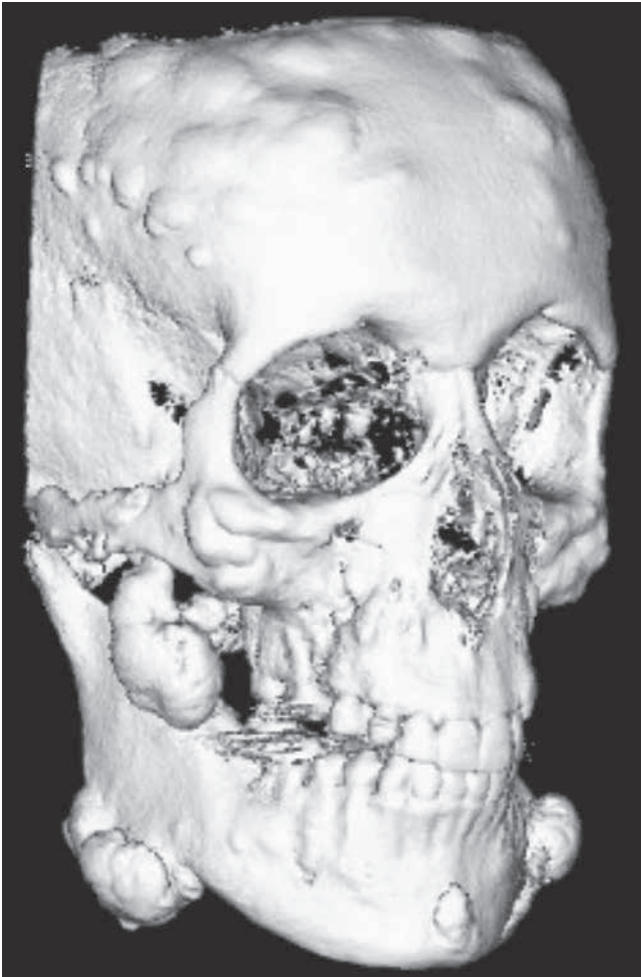
necessary information. Follow-up CBCT can also be justified then as the radiation dose is very low (Fig. 7). Other indications are diagnosis and follow-up of benign sinus and nasal cavity lesions (Fig. 8). The weakness of CBCT is that its "contrast resolution" is bad and that consequently the soft tissues cannot be evaluated. That is why a CBCT should be avoided in patients with a suspect lesion or proven malignant tumor (Fig. 9) or in patients presenting with neurological signs and/or deficits. In these patients the imaging modality of choice is MR. A large population has sinusitis and they of-

ten require repetitive imaging. This explains the fast increase in the number of CBCT "sinus" studies accounting today for almost 38% of all the CBCT studies in our hospital. These CBCT sinus studies substitute the sinus studies on MDCT which increases the availability of these more expensive MDCT systems for more complex CT examinations.

CBCT of the temporomandibular joint

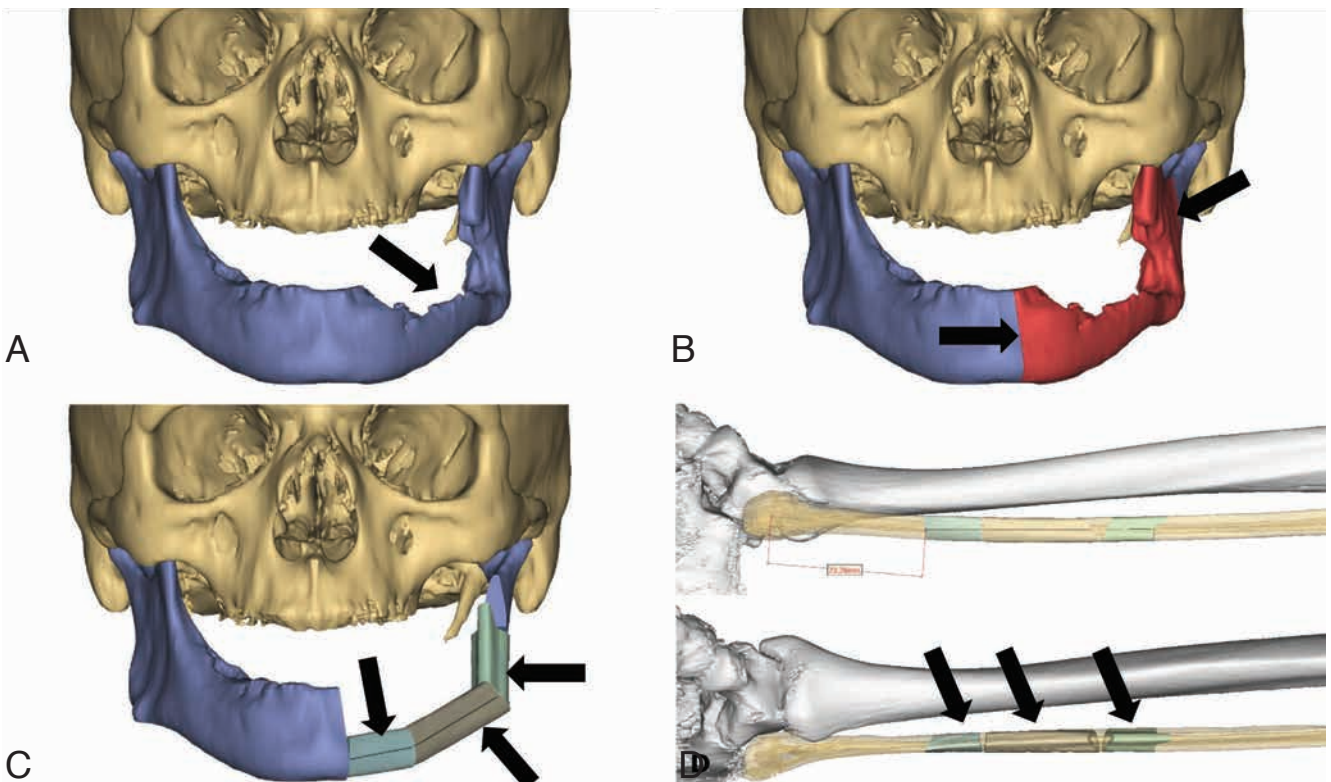
For many years conventional X-ray's were used to get a view on the temporomandibular joints (TMJ's).

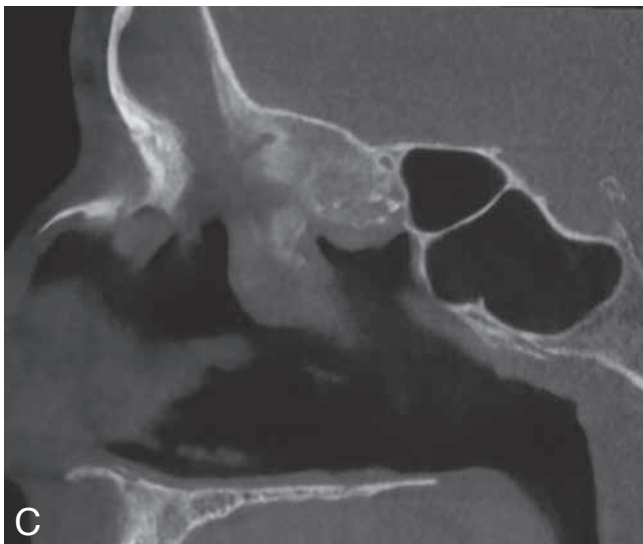
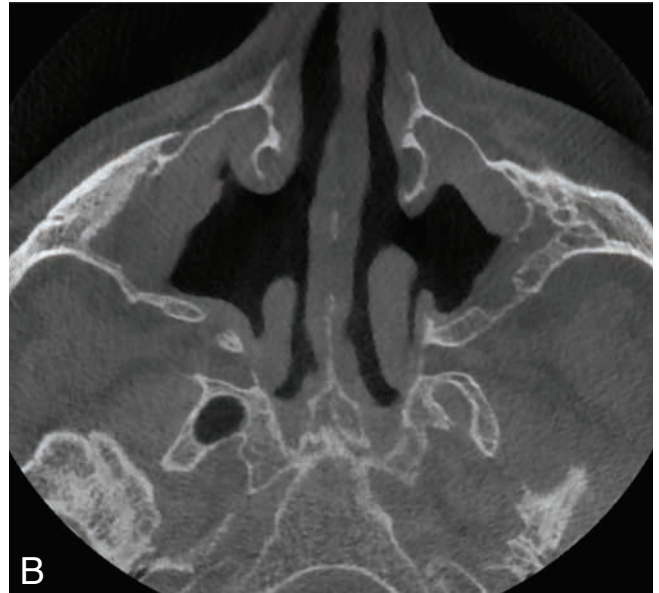
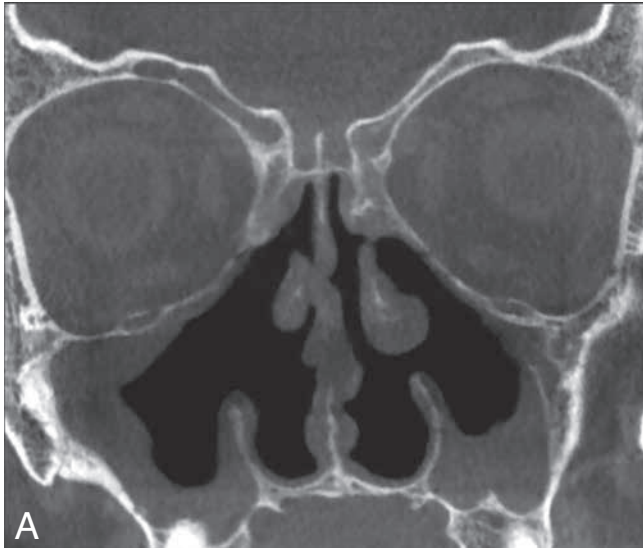
Lateral oblique transcranial (Schuller's), posteroanterior (Towne's) and caudocranial (Hirtz) views were very popular but were not always easy to acquire because of superposition of different structures on these 2D projection images. This explains why condylar fractures were one of the most missed fractures at that time. This problem was solved when CT and later MDCT were used to study the TMJ's. On these 3D-images superposition of bony structures was of course no longer a problem but this was achieved at the cost of a higher radiation dose. With the advent of CBCT this radiation dose



←
Fig. 3. — Patient with Gardner’s syndrome
 Three dimensional CBCT with reconstruction of the face and anterior skull showing the multiple osteomas which are typically found in patients with Gardner’s syndrome. These patients require repetitive imaging and hence low radiation dose CBCT is the perfect tool to keep the radiation dose low while providing 3D anatomical information.

↓
Fig. 4. — Oral cavity squamous cell carcinoma with mandibular destruction, pre-operative planning.
 A: Pre-operative diagnostic CBCT showing the mandibular destruction (arrow). B: Selection of the region which should be resected and reconstructed (red) (arrows). C: Computer simulation of the mandibular reconstruction, using bone grafts (arrows). D: Computer simulation of the fibular graft donor site on 3D MDCT images of the lower leg (arrows).



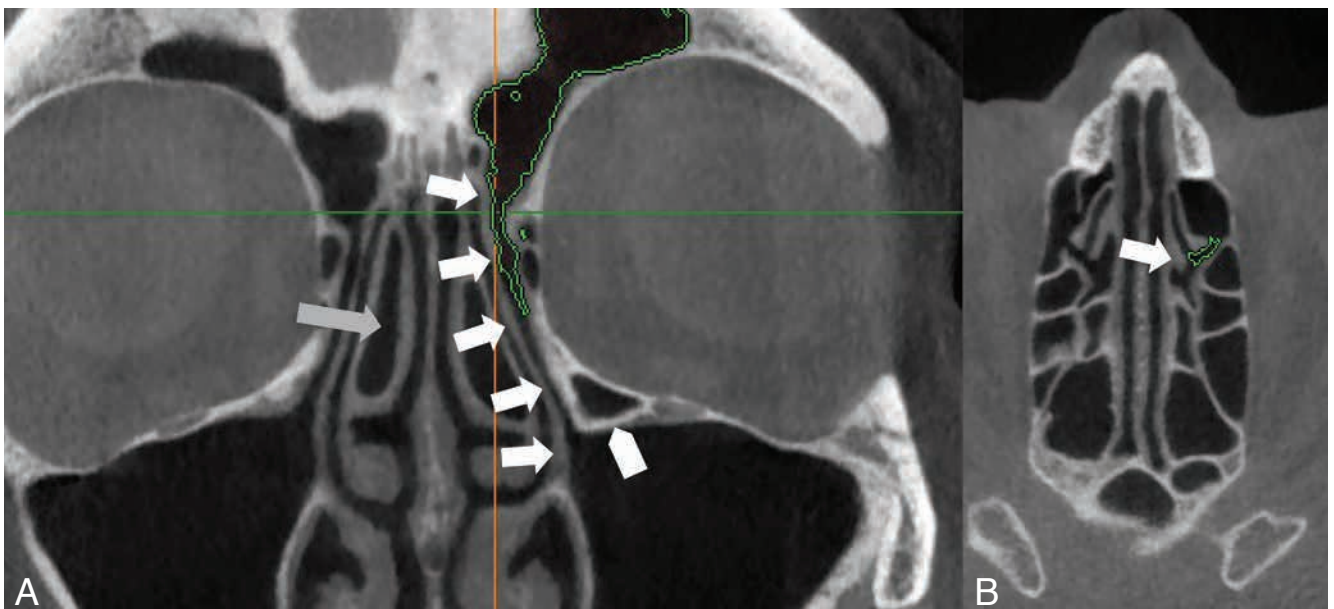


←
Fig. 5. — Status after bilateral FESS in patient with chronic sinusitis.

A-C: Coronal (A), axial (B) and sagittal (C) CBCT of the sinuses using a 8 x 8 cm FOV and a spatial resolution of 125 µm. Bilateral removal of the inferior turbinate, uncinate process, part of the medial wall of the maxillary sinus and major part of the ethmoid sinus. Bilateral remaining mucosal thickening and thickened appearance of the maxillary sinus walls confirming the "chronic sinusitis".

↓
Fig. 6. — Anatomy of the frontal sinus drainage – preoperative assessment.

A: Coronal 8 x 8 cm FOV CBCT with a spatial resolution of 125 µm. The uncinate process (white arrows) is attaching medially. Computer identification of the drainage pathway (green surface) shows that the frontal sinus drainage passes lateral to the uncinate process. If the frontal recess opens laterally to the uncinate process then an attempt to find the recess medial to the ethmoidal process would potentially lead to the olfactory fossa or the frontal lobe! Concha bullosa (grey arrow). Haller cell (white arrowhead). B: Axial CBCT image made at the level of the horizontal line on image Fig. 6A. Uncinate process (white arrow), frontal sinus drainage pathway (green surface).



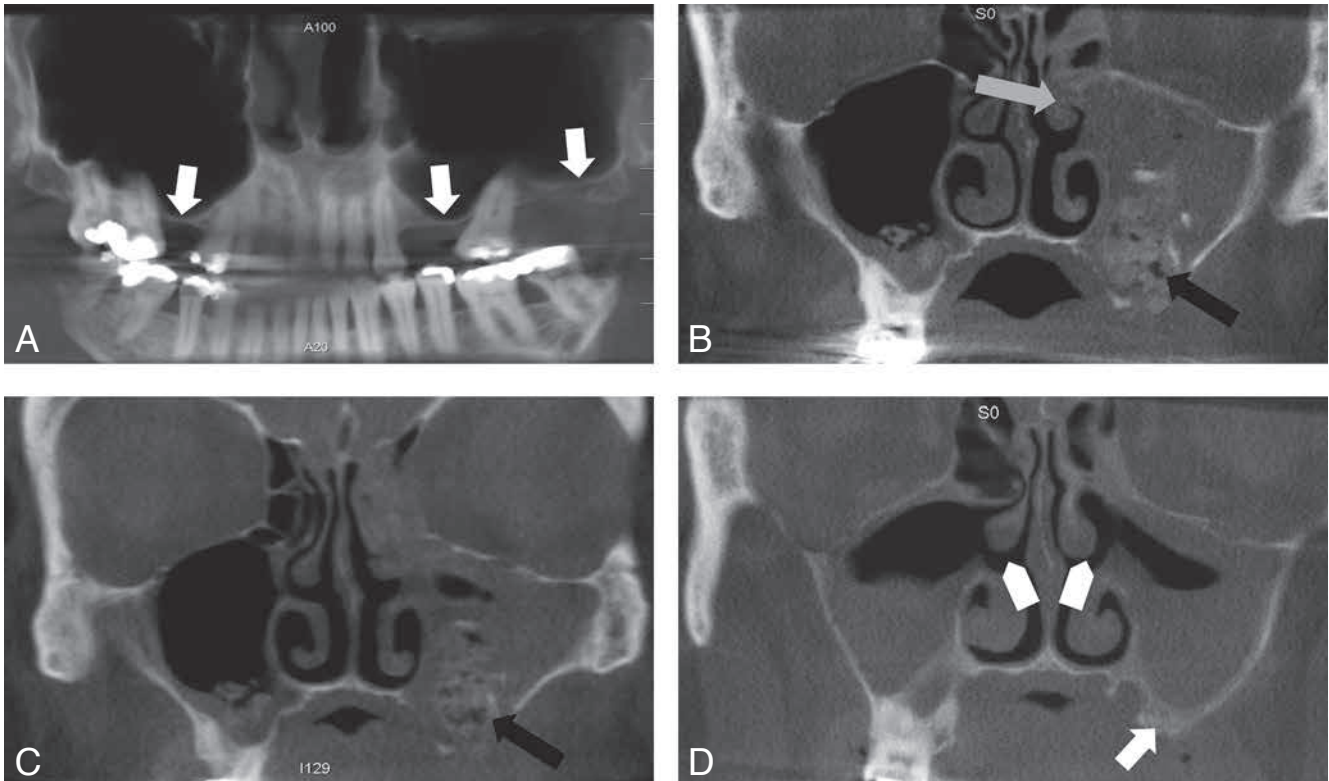


Fig. 7. — Repetitive imaging of the sinuses illustrating the need of “low dose” sinus imaging.

A: Presurgical CBCT dentascans for planning of implant placement showing an insufficient height of the alveolar ridge on both sides (white arrows). The sinuses are incompletely visualized and the OMU cannot be assessed. B: CBCT of the sinuses performed 6 weeks later after a sinus lifting procedure was performed on both sides. On the left side the procedure is complicated by infection (black arrow) and the complete sinus is inflamed and now the OMU can be evaluated but a clear opening to the middle meatus cannot be recognized (grey arrow). C: Follow-up CBCT of the sinuses after 8 weeks showing that the inflammation cannot be controlled conservatively (black arrow). D: Follow-up CBCT of the sinuses after 26 weeks. The infected material used for the sinus lifting was removed and a bilateral FESS procedure was performed (white arrowheads). There is healing of the left alveolar ridge (white arrow) but there is still partial obliteration of both sinuses which needs treatment before a new attempt of sinus lifting is possible.

could be further reduced. This made CBCT the technique of choice to study bony pathology of the TMJ (17). The most frequent indications today to perform a CBCT of the TMJ are: osteoarthritis (Fig. 10), inflammatory arthritis, synovial chondromatosis, fractures (Fig. 11), ankylosis, developmental abnormalities, benign neoplasms etc. (18). The low radiation dose also made CBCT suited to perform follow-up studies for the evaluation of disease progression or treatment results. CBCT with a 15 cm FOV in the axial plane allows visualization of both TMJ's (19). However, TMJ pain and internal derangement is most often caused by a disc problem. The soft tissues of the TMJ and the disc cannot be visualized by CBCT and hence internal derangement problems should be studied using (pseudo)dynamic MR.

Maxillofacial and nose trauma

CBCT is well suited to detect maxillofacial and orbital fractures and its

very high resolution and low radiation dose make it a better adapted imaging technique than MDCT. Moreover CBCT images have the same high quality in all possible planes, while the quality of the reformatted MDCT images is lower than the quality of the original in-plane axial MDCT images. This advantage of CBCT is best seen in patients with fractures at the level of the cribriform plate, orbita roof (Fig. 12) and orbital floor (Fig. 13) (20) which are easier to detect on coronal and sagittal CBCT images. This also explains why CBCT is very helpful in patients with CSF rhinorrhea where small fracture lines or breaches in the anterior or middle fossa must be detected. On the other hand CBCT has a very bad contrast resolution and therefore blood or soft tissue damage can hardly be evaluated. This explains why CBCT should no longer be used when clinical examination reveals potential intracranial, skull base or cranial nerve damage. Epidural and subdural hematomas, cerebral concussion and

bleeding, cranial nerve damage, intraorbital or globe lesions etc. can all be overlooked on CBCT and therefore these patients should immediately be referred for a MDCT or MR examination. Another CBCT indication is the evaluation of nose fractures. It is known that nasal fracture lines are missed on lateral and anteroposterior conventional X-ray's in up to 50% of the cases. False positive diagnoses are caused by nasal fissures, false negative diagnoses by lateral wall (Fig. 14) and cartilage fractures which cannot be distinguished on these images. The latter have however consequences as patients with nasal septum damage need an open reduction procedure. The most frequent reason to use imaging in patients with nose fractures are the medico-legal context (52%), the “diagnostic” reason for the referral (29%), the detection of trauma related foreign bodies etc. But, as mentioned, 2D X-ray's are often false negative and fractures or lesions of the septum and lateral nasal walls

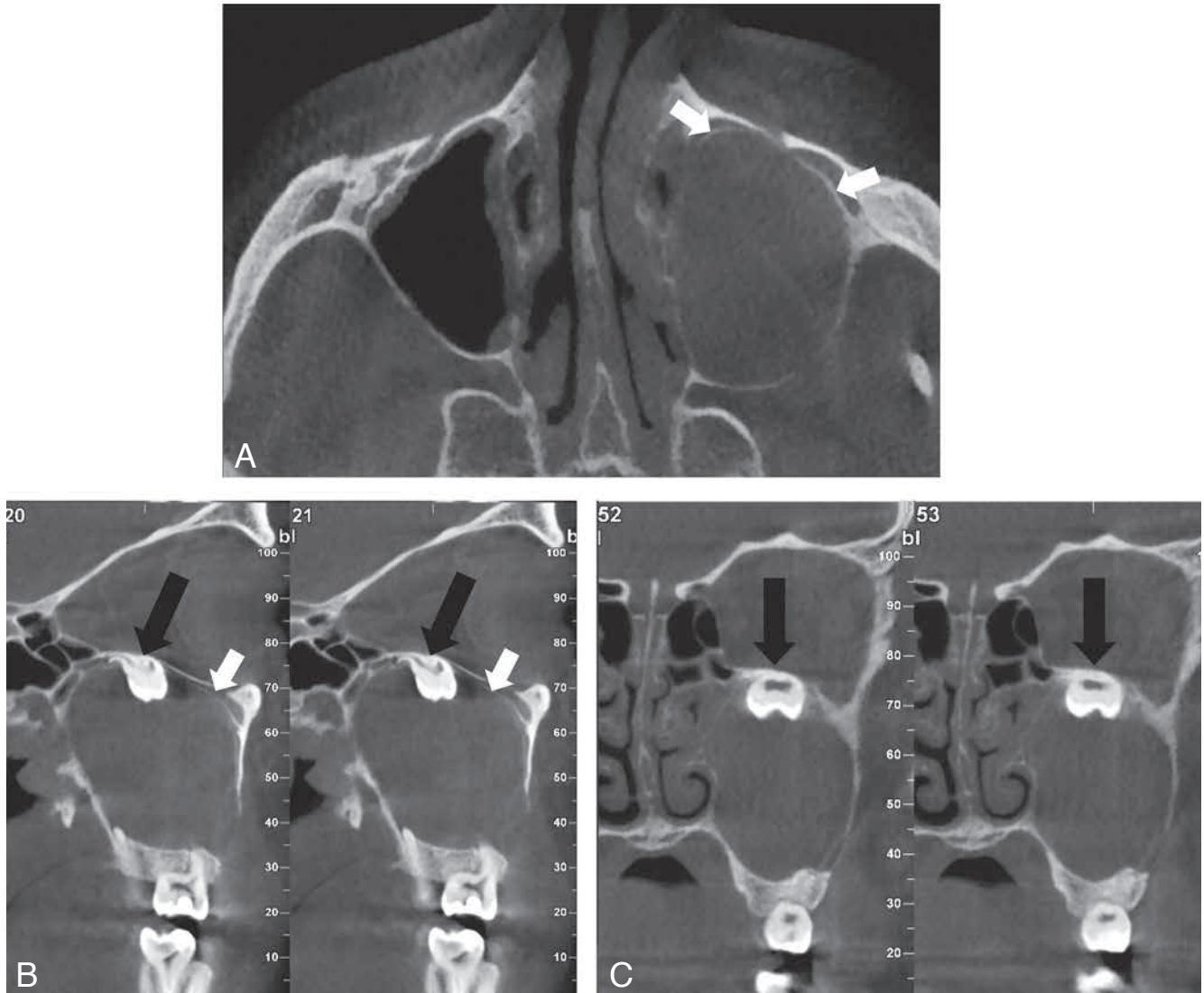


Fig. 8. — Maxillary sinus disease of odontogenic origin – keratocyst.

A: Axial CBCT of the sinuses showing that the left maxillary sinus is completely opacified. The cortical lining of the lesion inside the walls of the maxillary sinus reveals that the lesion is of odontogenic origin (white arrows). B: Sagittal CBCT images through the left maxillary sinus showing the cortical wall of the keratocyst (white arrows) and the upward displacement of the molar tooth, squeezed against the orbital floor (black arrow).

C: Coronal CBCT images confirming the displacement of the molar tooth (black arrow).



Fig. 10. — Osteoarthritis of the left TMJ.

A: Sagittal CBCT of the right TMJ showing a normal joint space (white arrow) and condyle.

B: Sagittal CBCT of the left TMJ with sclerosis of the condyle and an anterior osteophyte (grey arrow) and narrowing of the joint space (black arrow). C: Coronal CBCT of both TMJs. Normal joint space on the right side (white arrow), narrowed joint space (black arrow) and anteromedial condylar osteophyte on the affected left side (grey arrow).

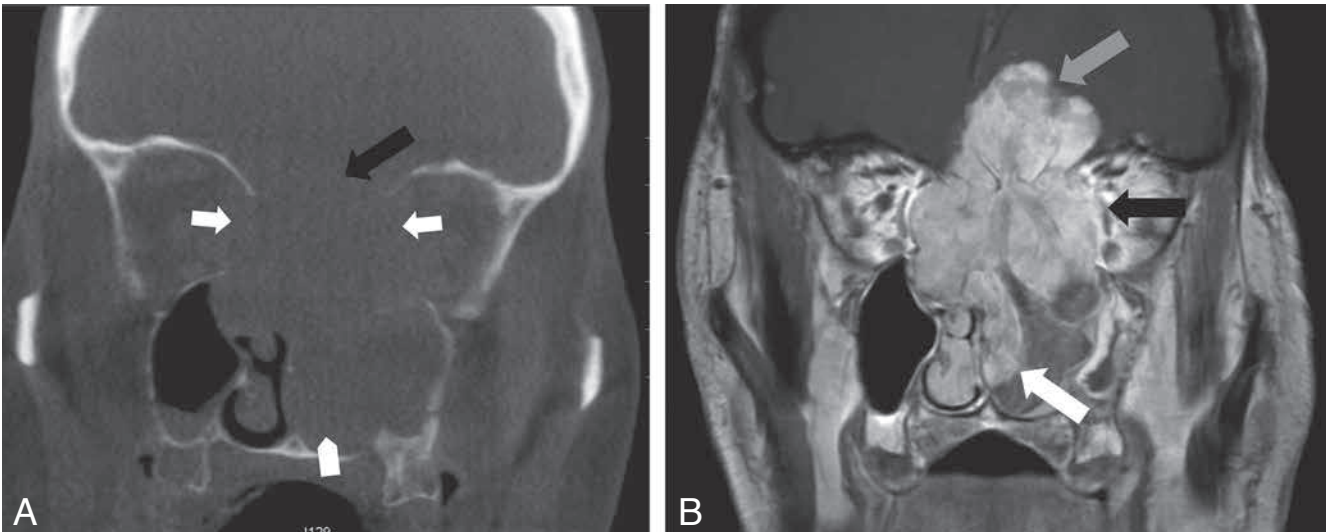
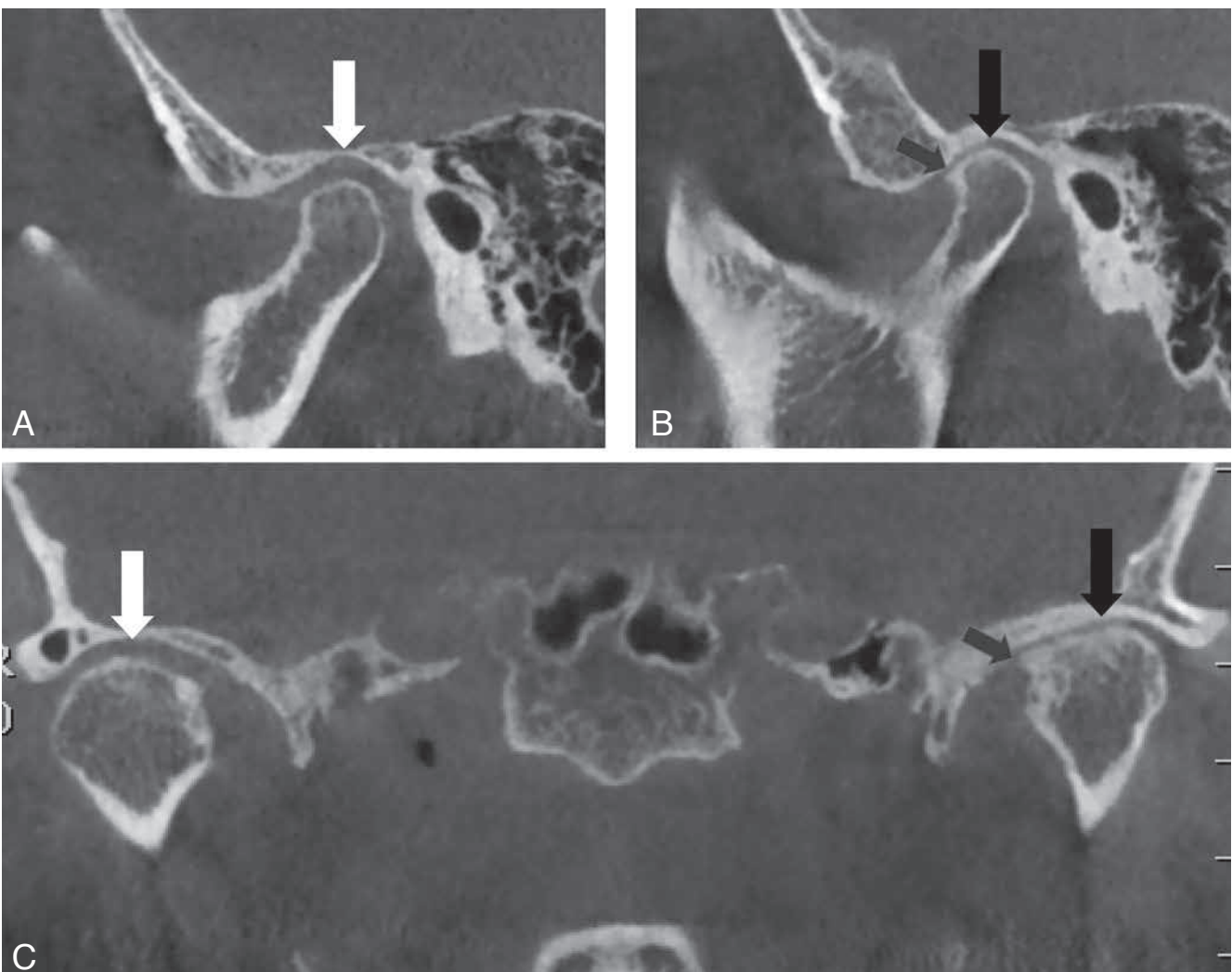


Fig. 9. — Inability of CBCT to visualize soft tissue lesions – squamous cell carcinoma of the ethmoid sinus invading the frontal lobes.

A: Low dose (32 μ Sv) coronal CBCT of the sinuses with a spatial resolution of 400 μ m. The destruction of the ethmoid cells, medial orbital walls (white arrows), and floor of the anterior fossa is obvious, however the extension of the tumor in the anterior fossa (black arrow) and nasal cavity (white arrowhead) cannot be assessed. B: Coronal gadolinium-enhanced T1-weighted MR image through the sinuses and anterior fossa showing the tumor extension in the anterior fossa (grey arrow), in the extraconal space of the left orbit (black arrow) and the extension down to the inferior meatus on the left side (white arrow).



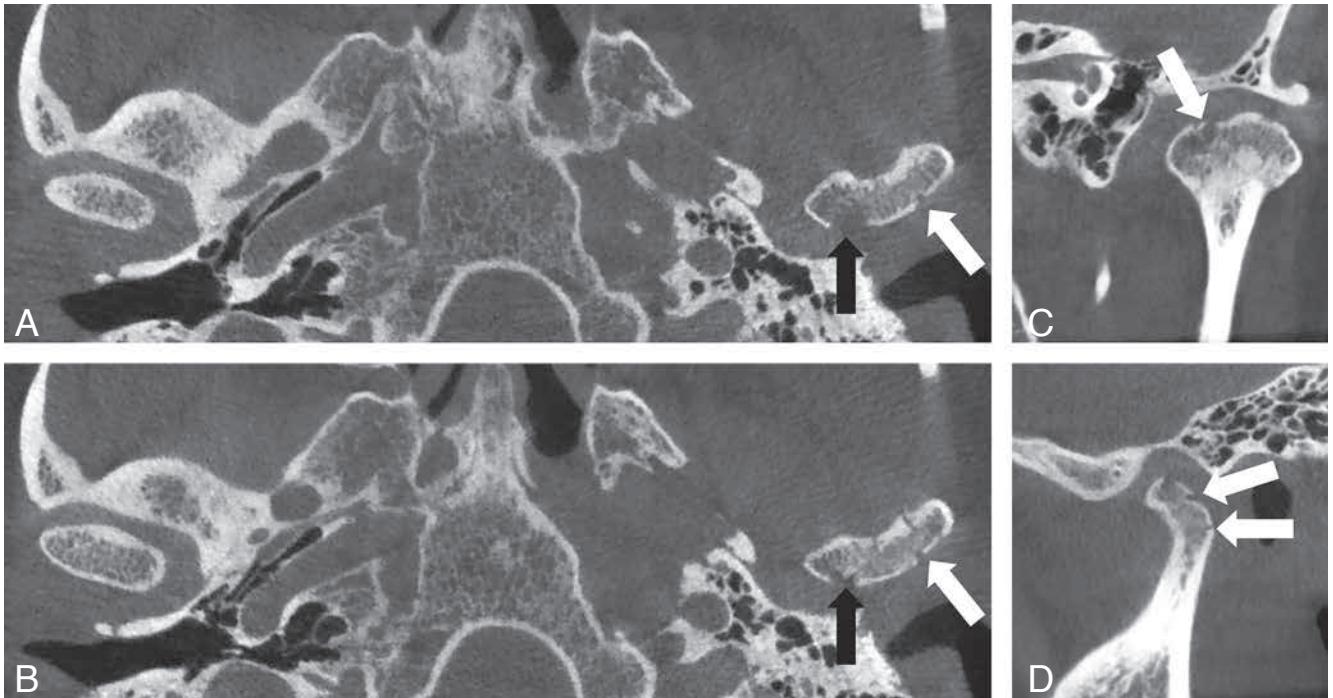


Fig. 11. — Undisplaced fracture of the left condyle.

A-D: Axial CBCT image at the level of the upper (A) and lower (B) part of the condyles and coronal (C) and sagittal (D) CBCT image through the left condyle showing the intact condyle on the right and the fractures through the cortex of the left condyle (arrows) without any displacement of the latter.

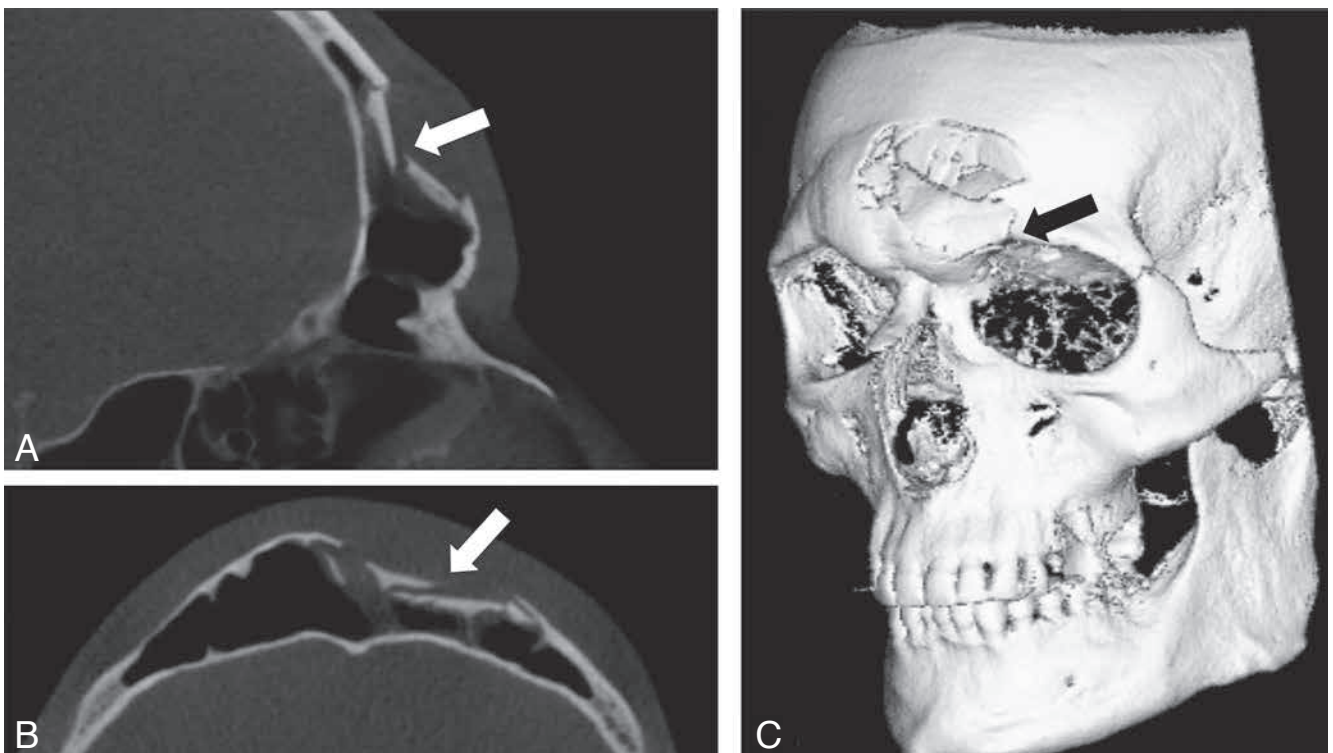


Fig. 12. — Fracture through the anterior wall of the frontal sinus with extension in the orbital roof.

A-B: Sagittal (A) and axial (B) CBCT image showing an impression fracture of the anterior wall of the frontal sinus (white arrows). C: Three-dimensional virtual reality CBCT reconstruction of the face showing the complex impression fracture of the frontal bone with an extension in the left orbital roof (black arrow).

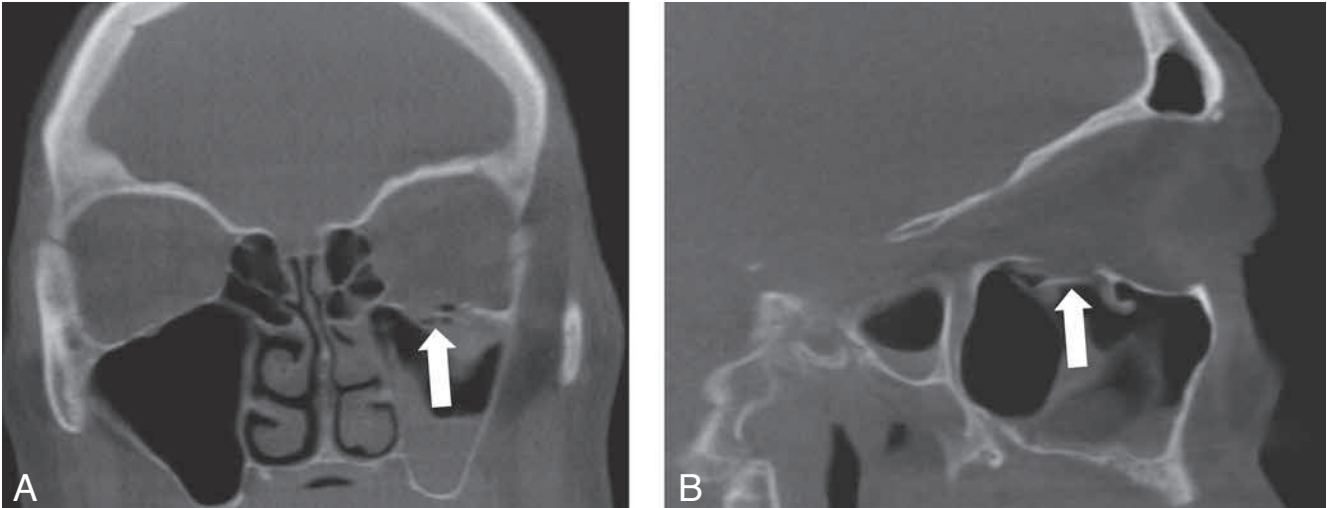


Fig. 13. — Fracture through the left orbital floor in a pregnant woman.
 A-B: Coronal (A) and sagittal (B) low dose CBCT (32 μ Sv) showing an inferior displaced segment of the orbital floor (white arrows). The small displaced segment is extremely well visualized even at the lowest irradiation dose and weakest possible resolution (0.4 mm) that can be achieved on CBCT. For further protection the patient was wearing a radiation protective coat during the examination.

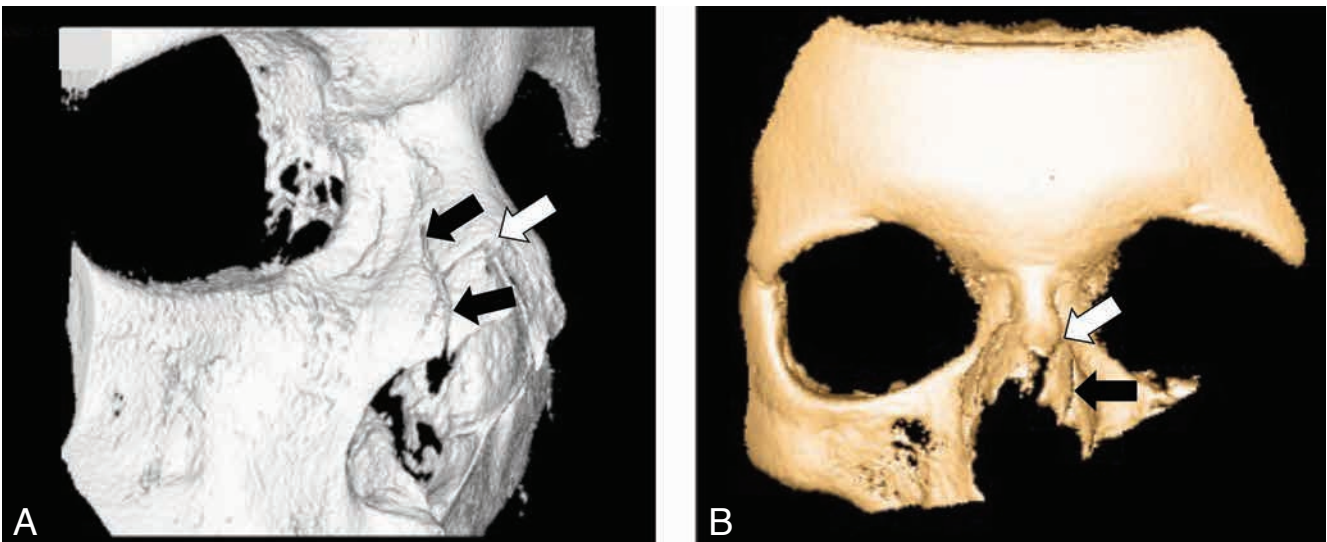


Fig. 14. — Nose fractures (two different patients).
 A: 3D virtual reality CBCT reconstruction of the nose showing 2 fracture lines running through the right lateral wall of the nose (arrows). B: 3D virtual reality CBCT reconstruction of the nose showing a fracture through the bridge (white arrow) and the left lateral wall (black arrow) of the nose.

are more missed than detected (21). 3D imaging techniques are able to detect most of these fractures which remain invisible on the 2D X-ray's. Nevertheless the use of conventional CT and MDCT was rejected because the much higher radiation dose did not match the questionable advantages, even in the more severe cases. The use of small FOV low dose 3D CBCT imaging changed this and it replaces today 2D X-ray imaging when imaging is needed or can be justified in these patients.

Skull base - vertex

Tumoral lesions of the skull base and vertex are best studied on MR. However, CBCT becomes valuable when calcifications inside the lesion must be demonstrated or excluded, and when a preoperative "bony" roadmap is required (Fig. 15, 16). Only the bone must be visible on these images and this explains why low dose high resolution CBCT can replace MDCT for these indications. Another indication to use low dose

CBCT is the evaluation of the thickness of the frontoparietal bone. This region is the harvest place for autologous calvarian split thickness bone grafts which are used to perform a "sinus lifting" or "bone augmentation" procedure in patients in whom not enough alveolar bone is available to warrant useful oral implant placement. These patients are scanned with their head and neck in anteflexion. In this position the upper jaw, the sinuses and the frontoparietal bone can be imaged together

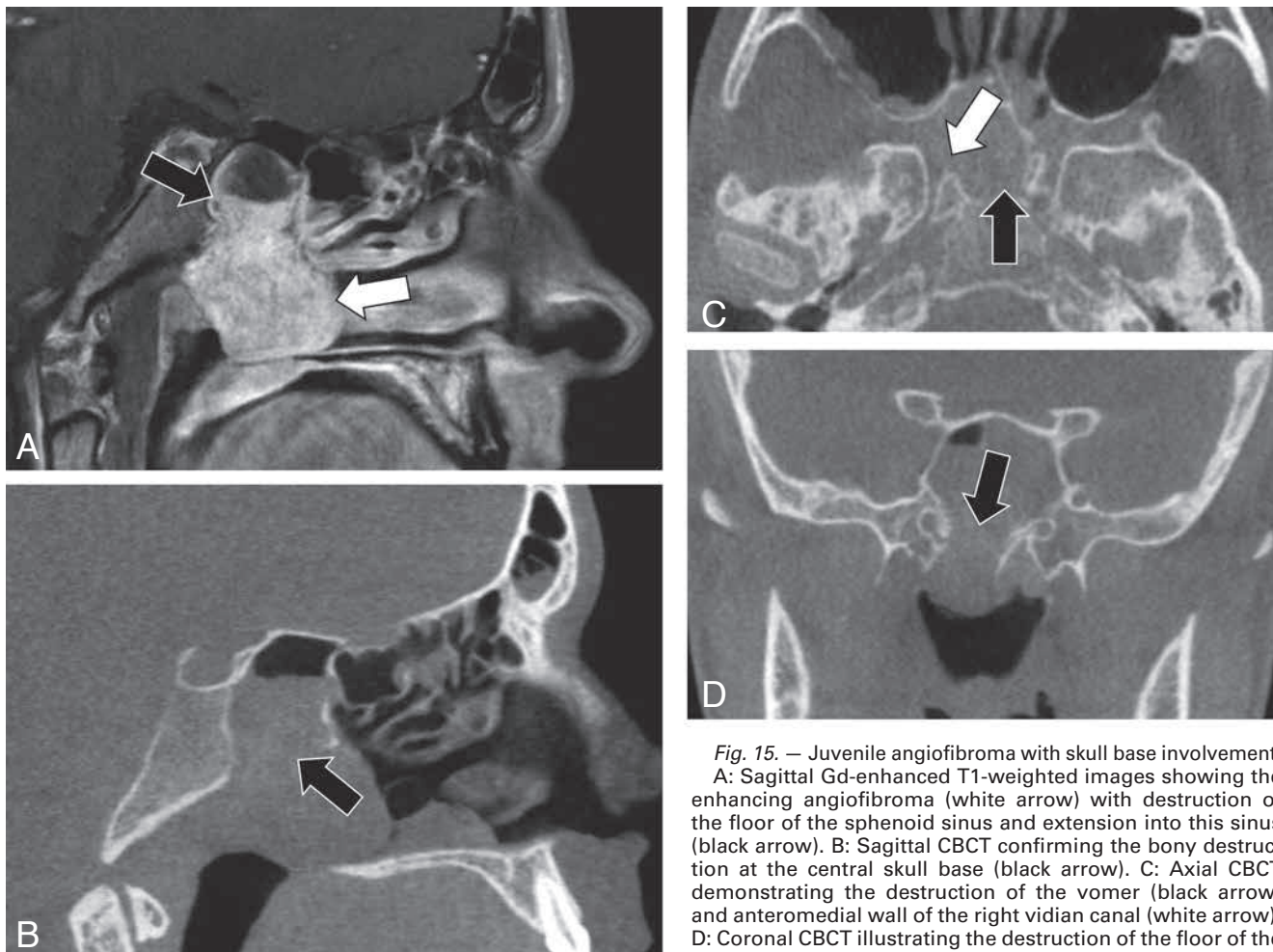


Fig. 15. — Juvenile angiofibroma with skull base involvement. A: Sagittal Gd-enhanced T1-weighted images showing the enhancing angiofibroma (white arrow) with destruction of the floor of the sphenoid sinus and extension into this sinus (black arrow). B: Sagittal CBCT confirming the bony destruction at the central skull base (black arrow). C: Axial CBCT demonstrating the destruction of the vomer (black arrow) and anteromedial wall of the right vidian canal (white arrow). D: Coronal CBCT illustrating the destruction of the floor of the sphenoid sinus (black arrow).

and hence the radiation dose is kept to a minimum while “dentascan” information about the maxilla, potential sinus problems (sinusitis, problems at the level of the OMU) and the “thickness” of the cranial donor site can all be assessed on one single CBCT study (22). Once the grafts are taken from the donor site the latter is filled up with hydroxyapatite, lyophilised bone, or with pharmaceutical products like Palaco® or Norian® (Fig. 17)

Swallow test - pharyngography

During a CBCT study 360 images are taken during the routine 20 second 360° rotation of the X-ray tube and flat panel detector around the patient’s head. This means that 18 images per second are acquired. This is a lot more than the 6-8 images/sec that can routinely be acquired with standard X-ray equipment and approaches the dynamic resolution

of videofluoroscopy. Videofluoroscopy is today the imaging technique of choice to perform barium/Gastrografin swallow tests and pharyngography but is expensive and unavailable in many hospitals. In these hospitals CBCT might become a good alternative for a videofluoroscopy swallow study or video pharyngography. The dynamic resolution of CBCT remains inferior to that of videofluoroscopy but its spatial resolution is higher (Fig. 18) while the radiation dose, 50 μ Sv for 18 images/second is lower than that of the conventional dynamic X-ray techniques which is 75 μ Sv for 6 images/second. Therefore one must be able to halt the CBCT rotation during the acquisition of the 360 images. This is today only available on some modified CBCT systems on which the feasibility was tested. It goes without saying that only CBCT systems made to study patients in the sitting position can be used for this application. The

results were excellent and it is clear that this technique has the potential to become the imaging technique of choice for sites where videofluoroscopy is not available. The major drawback is that the FOV only allows visualization of the oral cavity, nasopharynx, oropharynx, hypopharynx and larynx region and that the thoracic esophagus is not visualized. Therefore this technique cannot be used when the entire course of the oesophagus must be assessed but is ideally suited to perform pharyngographies.

Temporal bone imaging

Imaging of the temporal bone is challenging. The structures to be studied are extremely small and are located in or are surrounded by extremely dense bone. For many years conventional CT and MDCT were the preferred imaging techniques but a high radiation dose was needed. In-

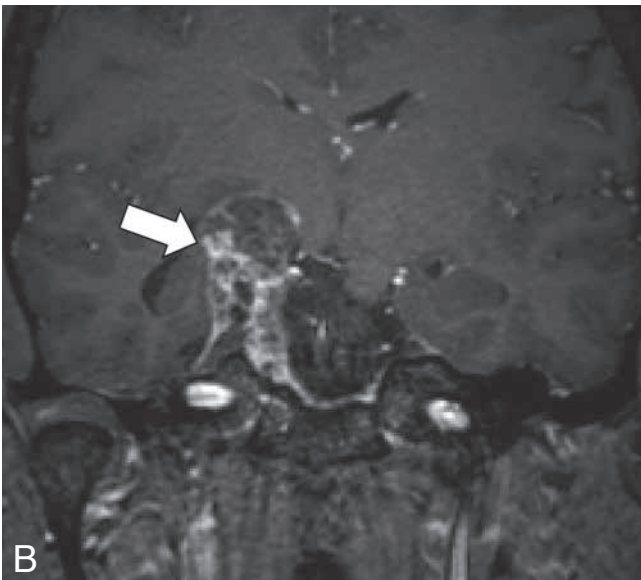
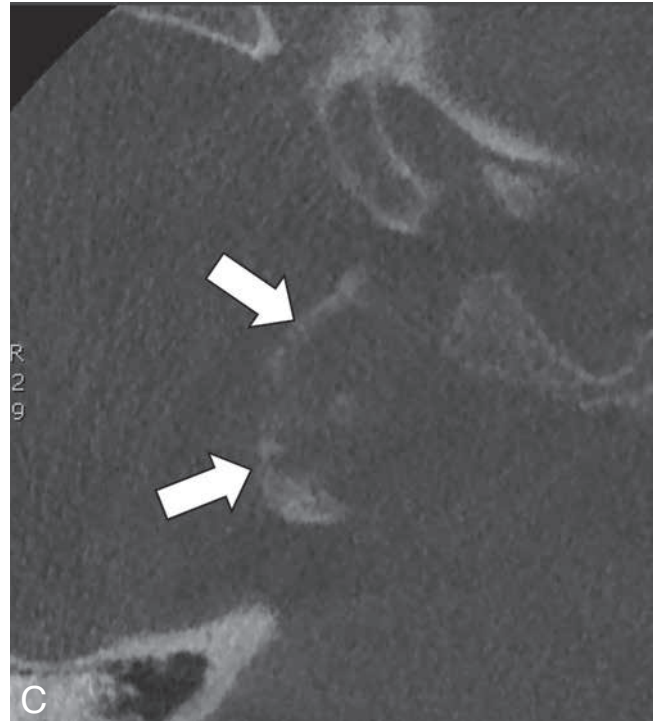
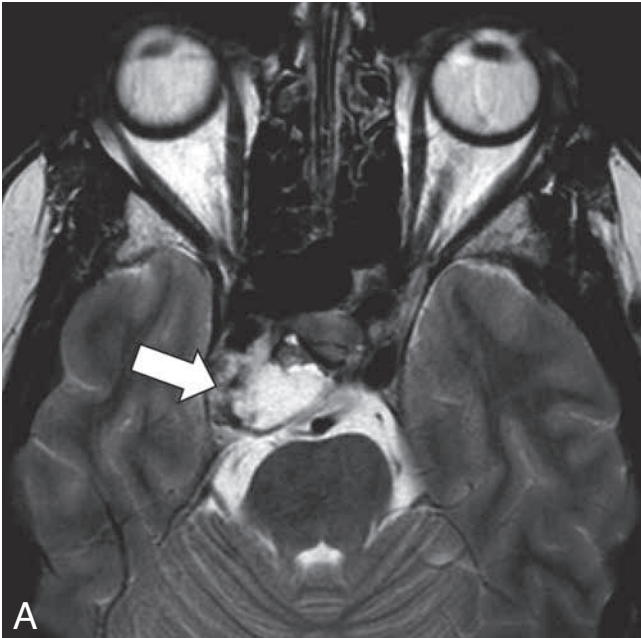


Fig. 16. — Chondrosarcoma with calcifications inside the tumor.
A: Axial T2-weighted images showing a lesion at the level of the right petro-occipital fissure with very high signal intensity (white arrow), compatible with a chondrosarcoma.
B: Coronal Gd-enhanced T1-weighted image through the lesions illustrates that it is a solid enhancing lesion (white arrow).
C: Low dose axial CBCT shows the presence of calcifications (white arrows), supporting the diagnosis of chondrosarcoma, a diagnosis which was later histologically confirmed.

deed, today temporal bone CT is probably one of the studies with the highest radiation burden. The resolution of these studies was situated between a routine moderate 625 μm and a highest achievable resolution of 230 μm . CBCT of course had the potential to acquire images with a better spatial resolution of 75 -150 μm at a lower radiation dose (23). Depending on the technique and MDCT system used the radiation dose can be reduced to 50% and in some cases even to 14% when CBCT imaging is used. Another advantage is that CBCT is less sensitive to metal artifacts from metal containing pistons and middle ear implants, cochlear implants or from metal artifacts coming from outside the

temporal bone (24-25)(Fig. 19). The major problem is however that this high resolution on CBCT can only be achieved with a long acquisition time of 40 seconds. This makes the technique vulnerable to movement artifacts and can result in the need for "retakes" resulting in a higher used radiation dose or even in a non-diagnostic study if the patients is not able to cooperate enough. Therefore the patient must be extremely well immobilized. This is more difficult in the sitting or standing position and therefore CBCT systems that can study the patients in the supine position are better suited for temporal bone imaging. The patients must also be instructed not to swallow and to breathe through the nose dur-

ing the scan as swallowing causes a movement of more than 100 μm and therefore severely degrades image quality. It is clear that small children and edentulous elderly patients or patients who are unable to co-operate enough are better studied using fast MDCT. In addition, more powerful X-ray tubes are needed to study the dense temporal bone structures. This is why today the best results are achieved when CBCT systems are used with an X-ray source which is able to deliver 110 kV and up to 10-20 mA. Even with these more powerful CBCT systems the image quality can still be degraded by noise when one is dealing with a "large or voluminous" head. In these patients it is wiser to go for a lower resolution of 150 μm providing images with a better contrast resolution and less noise. The development of more powerful CBCT systems could therefore again improve the quality of these temporal bone studies at a radiation dose lower or equal to the low dose protocols used today on the best MDCT systems. This would

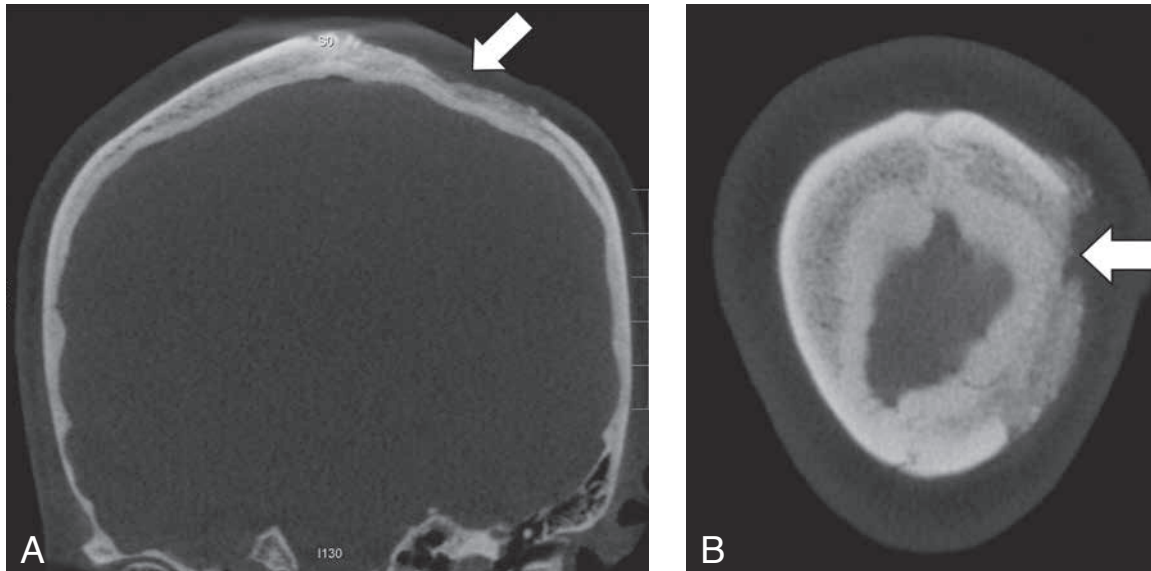


Fig. 17. — CBCT scanning protocol for preprosthetic cranial bone grafting of the atrophic maxilla Simultaneous CBCT imaging of the maxillary receptor site, sinuses and cranial donor site.

A: Coronal CBCT through the frontoparietal vertex with the head slightly in anteflexion. This allows simultaneous scanning and visualization of the maxilla receptor site, sinuses and cranial donor site. Harvest place (white arrow). B: Axial CBCT through the parietal skull, harvest place (white arrow).

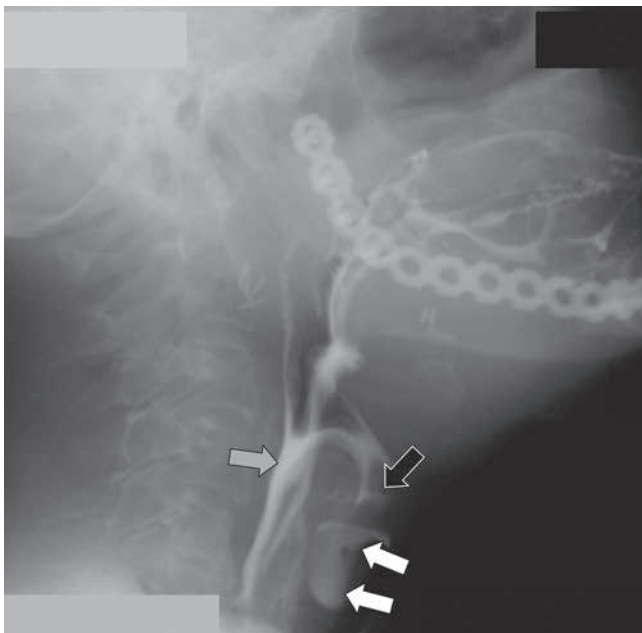


Fig. 18. — Dynamic CBCT, 18 frames per second, in a patient who underwent hemimandibular resection and reconstruction with a metal plate. The epiglottis shows a normal downward bending during swallowing (grey arrow) but in spite of this normal epiglottic function contrast is flowing down the trachea (white arrows). Contrast in the ventricle of Morgagni (black arrow).

be acceptable even at an equal radiation dose because the resolution and quality of the CBCT images would then be better than what can be achieved with MDCT in almost all patients. Moreover this could open the possibility of routine 75-85 μm imaging and/or faster acquisition (rotation) times. These more powerful systems are today only needed for temporal bone studies and some musculoskeletal (MSK) studies and are not needed for dental imaging. Hence access to these more powerful systems can then best be restricted to those users who are performing the above mentioned studies that might require a higher radiation dose. It is possible to image both temporal bones together (single rotation with a 15 x 5 cm FOV) or separately (two separated rotations with a 8 x 8 x 5 cm FOV). The radiation dose of both techniques is similar as is the image quality. In our experience the slightly higher resolution that is achieved when the temporal bones are imaged separately does

Fig. 21. — CBCT double oblique reformatted high resolution images (150 μm resolution) of the middle ear in two patients with a congenital middle ear malformation.

Stapedial artery (A), congenitally narrowed oval window/footplate (B).
A: CBCT image in a patient presenting with tinnitus on the right side, demonstrating the presence of a stapedial artery between the crurae of the stapes (black arrow). Normal thickness of the footplate (white arrow). Notice the presence of a ventilation tube in the thickened drum. B: CBCT image in a patient with congenital conductive hearing loss on the left side. The posterior part of the oval window or footplate is calcified and thickened (white arrow). Only the anterior 2/3 of the oval window and/or footplate are open (black arrow). Capitulum of the stapes with attachment of the stapedius muscle tendon (grey arrow).

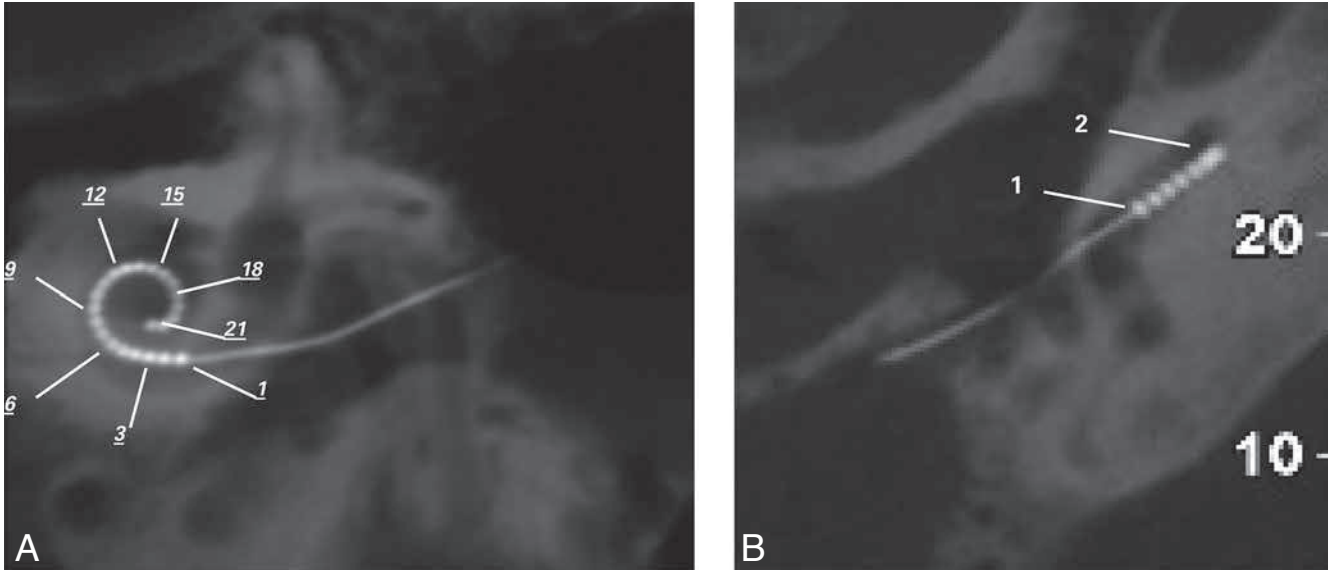


Fig. 19. — CBCT used to verify the position of a cochlear implant (Cochlear Nucleus Freedom with 22 electrode-array contact points).

A: Parasagittal CBCT reconstruction through the electrode array showing the 22 electrode contacts without any metal artefacts. Normal position inside the cochlea with the first electrode (1) inside the basal turn. B: Axial CBCT image through the basal turn of the cochlea demonstrating the normal position of the electrode array inside the scala tympani (1) with a normal open scala vestibuli (2).

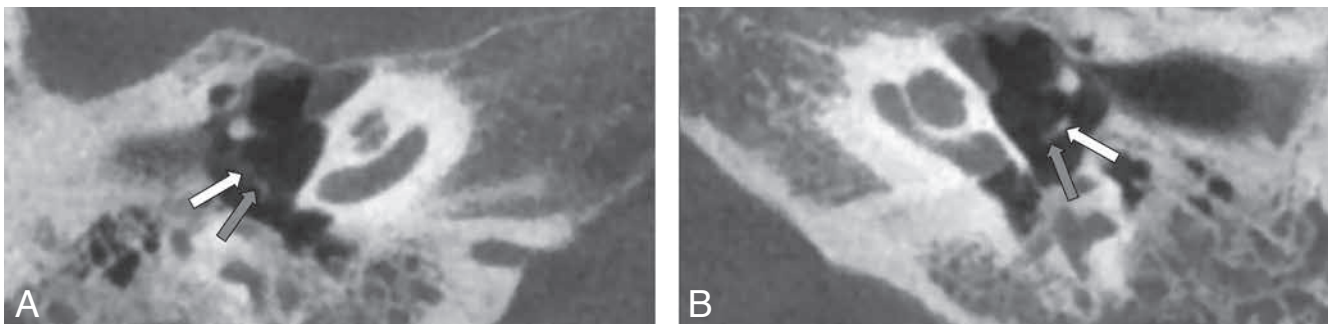
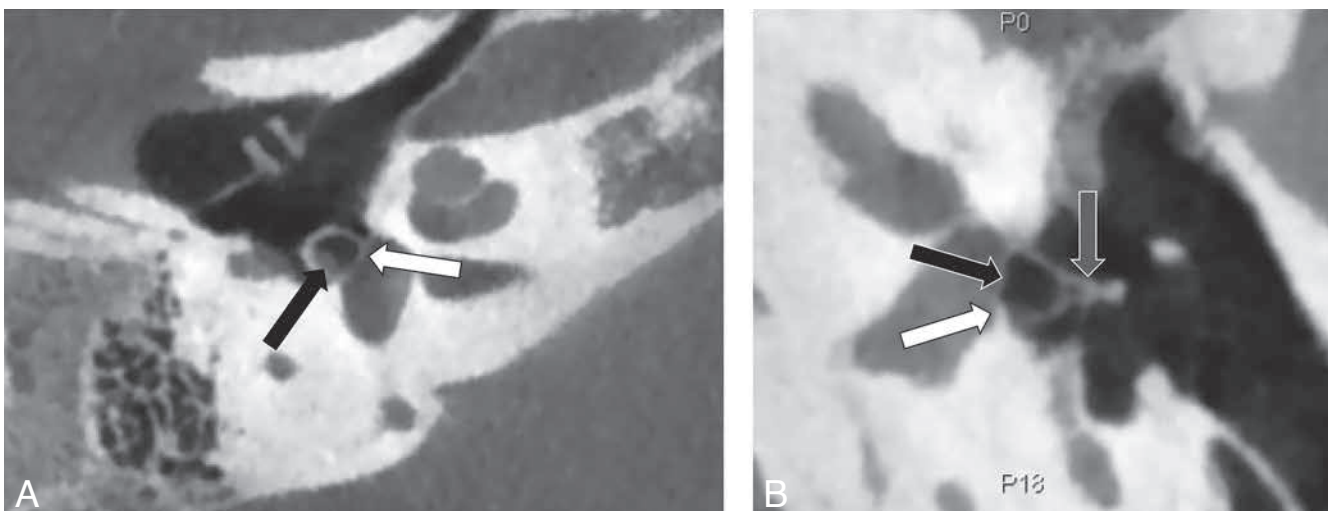


Fig. 20. — CBCT in a patient with conductive hearing loss: lysis of the incudostapedial junction on the right side.

A: Axial CBCT of the right middle ear with a spatial resolution of 150 μ m showing demineralization of the lenticular process of the incus (white arrow) and stapes capitulum (grey arrow). Surgery confirmed the findings and the ossicular chain was repaired. B: Axial CBCT of the left middle ear showing the normal mineralization of the lenticular process of the incus (white arrow) and stapes capitulum (grey arrow).



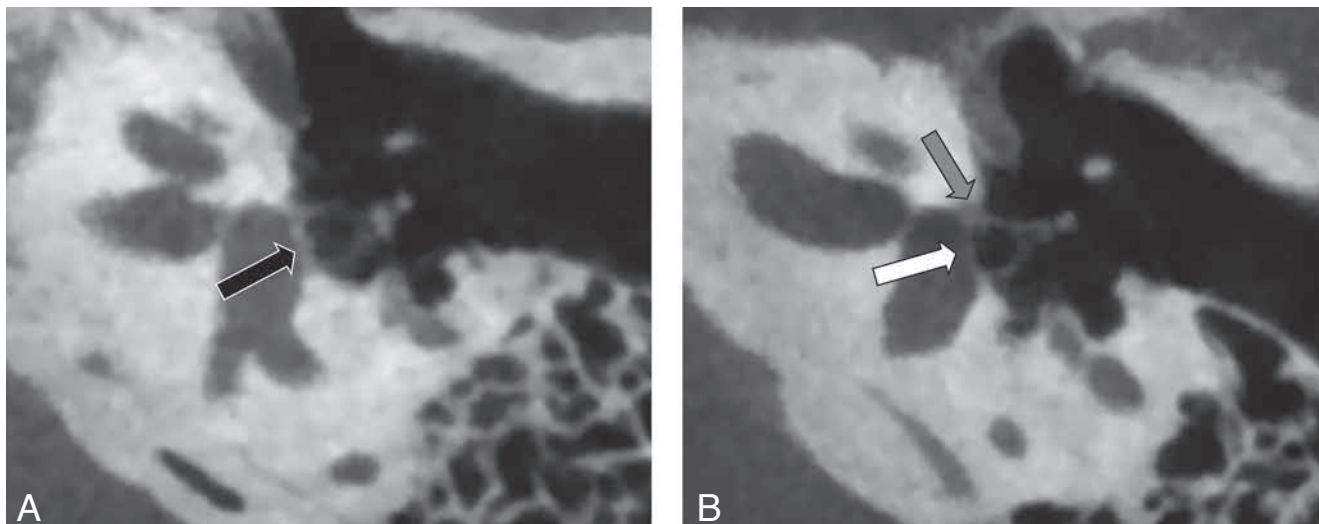


Fig. 22. — CBCT double oblique reformatted high resolution images (150 μm resolution) of the middle ear in two different patients with otosclerosis.

A: Fenestral otosclerosis with a thickened grayish appearance of the footplate (black arrow). The fissula antefenestram is normal. Type 1 (Veillon) otosclerosis. Compare with the normal thickness of the footplate in B. B: Fenestral otosclerosis with a hypodense otospongiosis area in the fissula antefenestram (grey arrow), just anterior to the footplate with a size of less than 1 mm. Type 2a (Veillon) otosclerosis. Normal thickness of the footplate (white arrow).

not justify the 100% more time that must be invested. Preliminary results of an ethical committee approved comparative study between CBCT and MDCT showed that the majority of the checked anatomic structures were better or even only seen on CBCT (20) and the superiority of CBCT over MDCT was more pronounced in the coronal plane. This is explained by the fact that the coronal MDCT images are reformatted and this is needed as the radiation dose in the axial plane is already relatively high making additional separate scanning in the coronal plane unacceptable. The higher resolution allows making diagnoses which could not be made or were more difficult to make with MDCT and apply for lesions of the external, middle and inner ear (26). In patients with chronic otitis media the lysis of the lenticular process or long process of the incus (Fig. 20), inflammatory changes between incus and malleus, subtle tympanosclerosis, incudostapedial luxation, the thin walls of the cholesteatoma sac fol-

lowing auto evacuation, etc. can all be seen on CBCT images. The higher resolution of CBCT also makes it easier to detect ossicular fractures, dehiscent facial nerve canals, congenital inner and middle ear malformations etc (Fig. 21). The diagnosis of a congenital middle and/or inner ear malformation frequently has to be made early in life and in these very young patients the CBCT study has to be performed under anesthesia, hence anesthetic gases must be available in the CBCT room. A MR study is most often also required for inner ear malformations which are then performed during the same anesthesia session. The major gain of CBCT over MDCT is in the detection of otosclerosis, stapes – stapes footplate – oval window (Fig. 22), and dehiscent superior semicircular canal lesions (Fig. 23). The subtle changes on the footplate or at the fissula antefenestram in otosclerosis, can sometimes only be detected on CBCT. The use of high resolution CBCT also allows detection of stapes, footplate/oval window abnor-

malities and lesions caused by congenital malformation (e.g. aplasia of the stapes or crura of the stapes, aplasia or hypoplasia of the oval window) by chronic otitis media (e.g. tympanosclerosis with calcifications on stapes and/or footplate), etc. Finally, the positive MDCT diagnosis of superior semicircular canal dehiscence or “third window) is often corrected as negative on CBCT as the very thin bony wall of the superior semicircular canal is only detectable on images with a resolution close to 100 μm . The above explains why CBCT has the potential to and is already replacing MDCT. The main reason why CBCT is not used for temporal bone imaging today are availability of a high quality CBCT (today only 3 to 4 CBCT systems have the quality to perform temporal bone studies), the longer acquisition time – computer calculation time – slower and more complicated workstation, and the less user friendly and more time consuming “PACS” connection. From the diagnostic and quality point of view CBCT is ready

→

Fig. 24. — Fracture of the lunate and scaphoid bone, missed on conventional X-rays. A-B: Axial 150 μm resolution images through the wrist showing a subtle non-displaced fracture through the anterior part of the lunate bone (white arrow) and through the posterior part of the scaphoid bone (black arrow) which could only be demonstrated on CBCT.

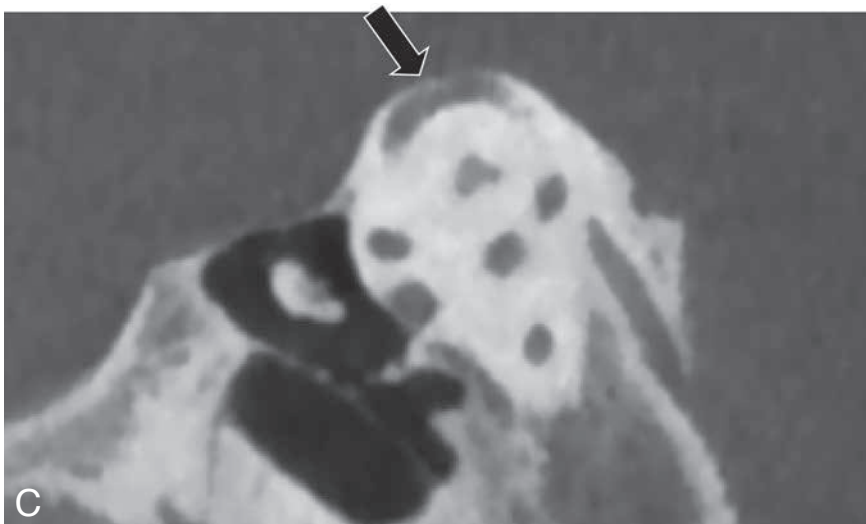
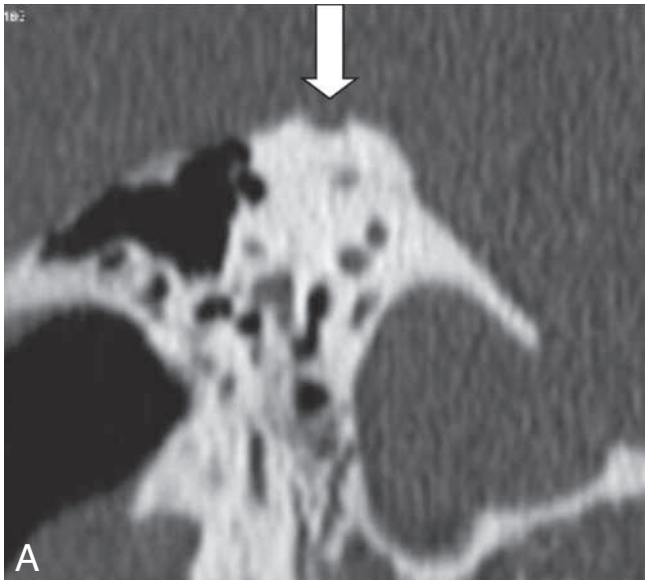
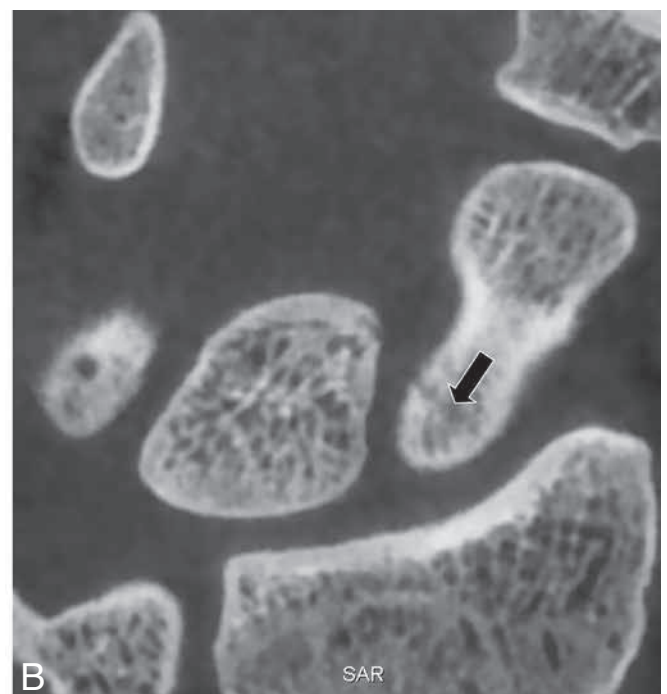
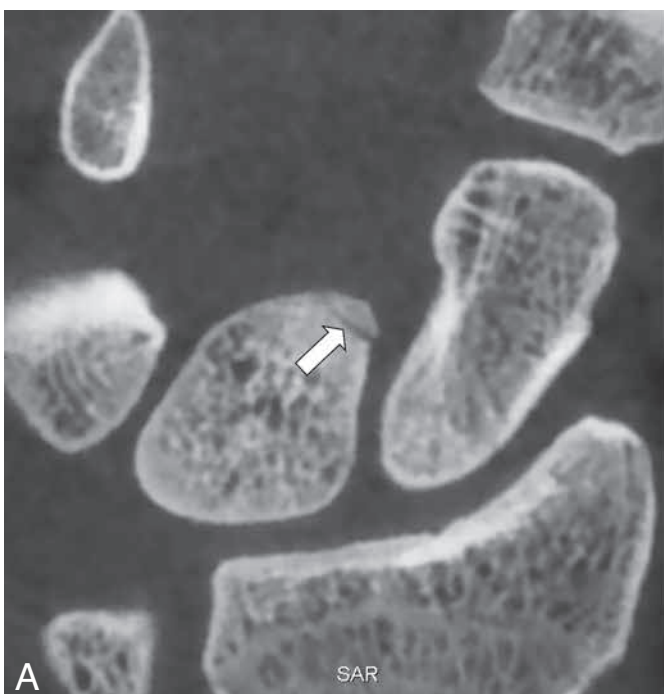


Fig. 23. — Dehiscent superior semicircular canal imaging: positive on MDCT, negative on CBCT

A: Reformatted coronal CT image shows a dehiscent superior semicircular canal (white arrow). In order to reduce the dose the patient was scanned in the axial plane and coronal reformatted images, with some loss of resolution as a consequence, were made.

B-C: Coronal (B) an paracoronal CBCT images parallel to the superior semicircular canal (C) with the same resolution (150 μ m) and quality as the axial images and which can therefore show the thin bony wall of the superior semicircular canal (black arrow).



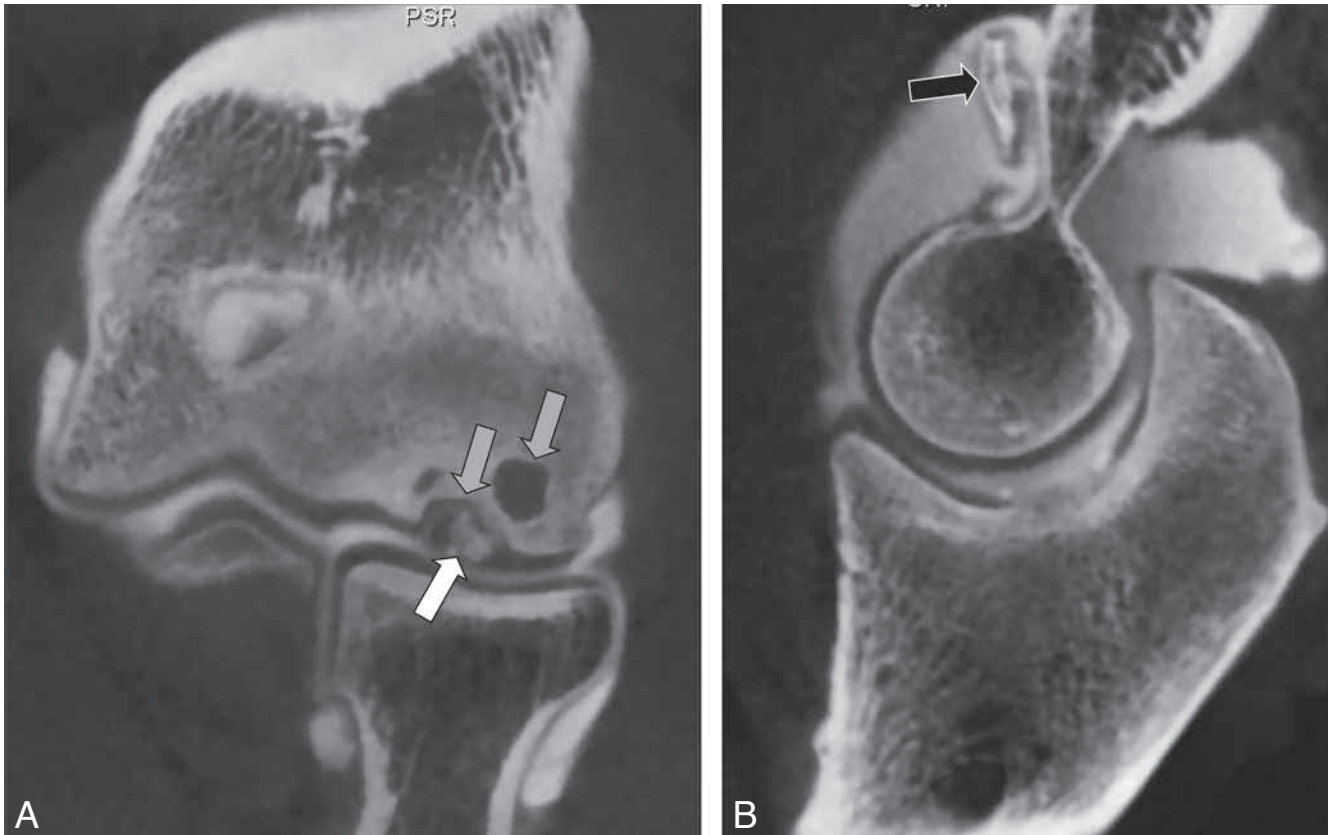


Fig. 25. — CBCT-arthrography in a patient with osteochondritis dissecans of the elbow.

A-B: Coronal (A) and sagittal (B) high resolution 150 μ m CBCT images through the elbow showing a loose body and the destroyed cartilage at the level of the capitulum of the humerus (white arrow) and a second loose body proximal to the trochlea (black arrow). Bone erosions/defects (grey arrows).



Fig. 26. — Non-union of a scaphoid bone fracture, follow-up after surgery.

Fractures through the scaphoid bone treated with a scaphoid bone screw. Notice the non-union of the fractures (white arrows) and the absence of metal artefacts.

to replace MDCT and its superiority will only increase with the ongoing technical improvements of CBCT systems.

Musculoskeletal imaging

Patients were examined in the sitting or standing position on almost all of the first available CBCT systems. Therefore the only MSK structure that was examined at that time was the cervical spine. However the initial CBCT systems couldn't provide the needed spatial resolution and quality to match the quality of MDCT. Even with the advent of more powerful CBCT systems the visualization of the lower cervical vertebra remained a problem. Even the latest most powerful CBCT systems are unable to deliver X-rays which can visualize the lower cervical vertebra after passing through the shoulders. Also the limited field of view makes visualization of the "entire" cervical spine difficult in larger patients. Nevertheless the newer high-end

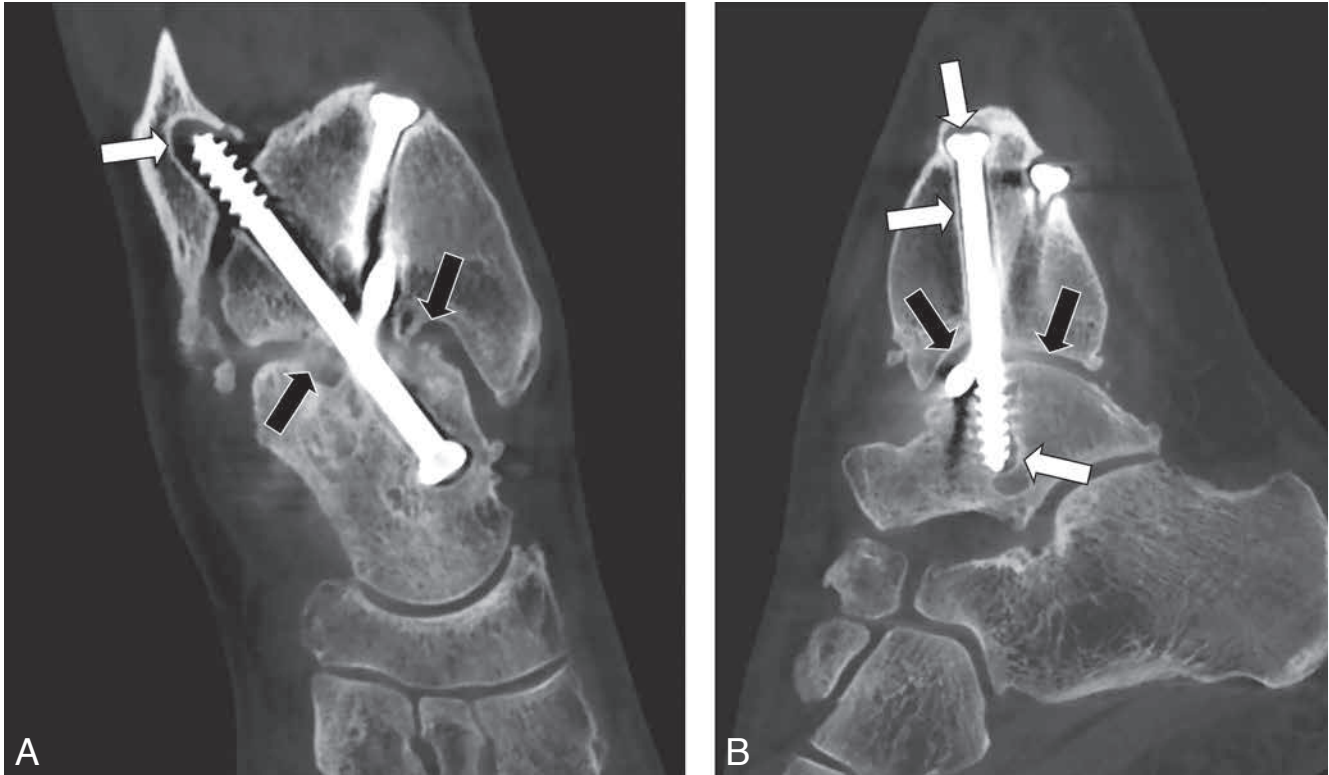


Fig. 27. — Follow-up study after arthrodesis procedure of the ankle. Coronal (A) and sagittal (B) high resolution (150 μ m) images of the ankle show the presence of three screws which are hardly disturbing the visualization of the surrounding bone. The joint space between the tibia and talus is still open (black arrows) and there is also bone resorption around the screws (white arrows) confirming the clinical doubt about normal evolution to arthrodesis.

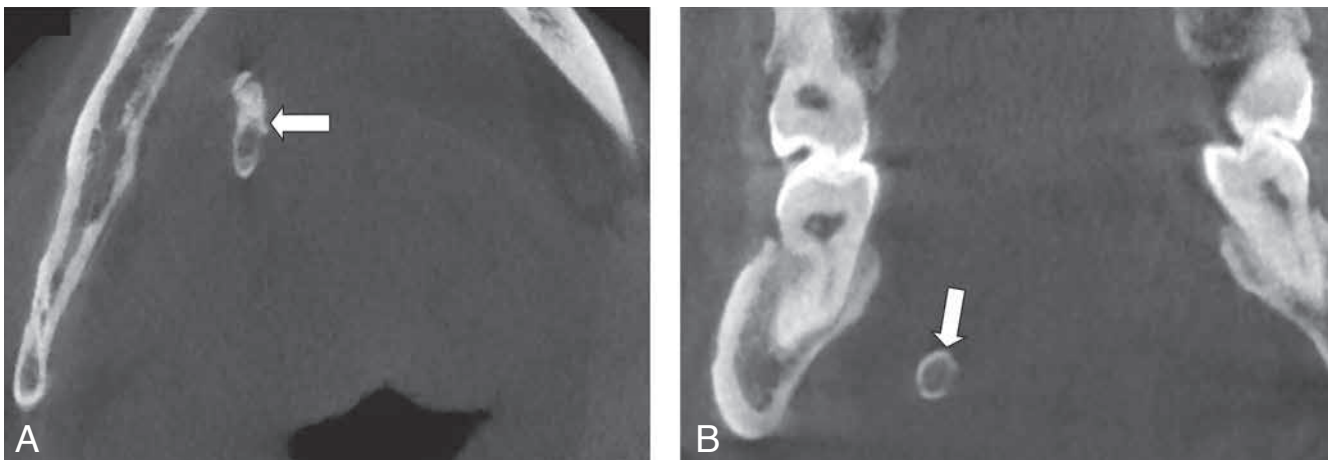


Fig. 28. — Sialolithiasis in Wharton's duct Axial (A) and coronal (B) CBCT through the floor of the mouth showing a duct stone in Wharton's canal (white arrows).

CBCT systems proved their value in the evaluation of local bone lesions and in difficult cases where metal artifacts on MDCT and MR make evaluation of the vertebra impossible. Musculoskeletal CBCT became possible with the advent of systems that looked like a small CT and that could examine the patient in the su-

pine position on a trolley or systems with a ring design through which an arm or leg could be put. Again resolution and image quality were very variable depending on the system. The best systems however offer 100-125 μ m high quality images of the fingers, wrist (27), elbow, foot, ankle and knee and are also able to image

long bones of the extremities, even when osteosynthetic bone-plates and screws are present (28). And above all this is achieved at a lower radiation dose than on MDCT. Hence CBCT is gradually replacing MDCT and MR replaces MDCT when soft tissue information is needed. Detection of fractures which are invisible

or doubtful on conventional X-rays, verification of healing fractures and non-union especially when osteosynthetic material is present (29), assessment of benign tumors and degenerative changes of the bony structures, arthrography (30) etc. are some of the excellent CBCT applications in the extremities and the above mentioned joints. Musculoskeletal CBCT is today already the fastest growing new indication and in the future more powerful systems using larger flat panel detectors could even increase the share of this application.

Miscellaneous imaging

A less frequent indication is the diagnosis of salivary gland calculi when ultrasound cannot solve this problem. The high resolution and low radiation dose make CBCT suited to detect these calculi (31). Moreover these calculi often occur in younger patients and in the areas close to the eyes, two reasons to go for the technique with the lowest radiation dose. CBCT sialography is another new possible technique (32). A different less frequent indication is dacryocystography. It is possible to put some iodine containing contrast material in the eye and to visualize the lacrimal canaliculi and sac with CBCT and to check if the nasolacrimal duct is patent. Again CBCT offers high resolution at a low radiation dose which is important in this area so close to the lens. CBCT is also used for 3D-analysis of the airway in patients with cleft lip and/or palate (33), obstructive sleep apnea (34) and in patients who underwent orthognathic surgery (35).

Endodontics - Periodontology

As described above, CBCT vendors developed high-end systems which enabled sinus, temporal bone and MSK imaging. The very high resolution that can be achieved with these systems in turn opened new possibilities in the endodontic and periodontal field. Visualisation of a fourth molar tooth root canal, tooth ankylosis, subtle dental fractures, evaluation of the dental development stage etc. are only some of the many new indications but this is beyond the scope of this "non-dental applications" paper.

References

1. Casselman J.W., Quirynen M., Lemahieu S.F., Baert A.L., Bonte J.:

- Computed tomography in the determination of anatomical landmarks in the perspective of endosseous oral implant installation. *J Head Neck Pathol*, 1988, 7: 255-264.
2. Jacobs R.: Dental cone beam CT and its justified use in oral health care. *JBR-BTR*, 2011, 94: 254-265.
3. Pauwels R., Beinsberger J., Collaert B., Theodorakou C., Rogers J., Walker A., Cockmartin L., Bosmans H., Jacobs R., Bogaerts R., Horner K.: The SEDENTEX CT project consortium: effective dose range for dental cone beam computed tomography scanners. *Eur J Radiol*, 2012, 81: 267-271.
4. Loubele M., Bogaerts R., Van Dijck E., Pauwels R., Vanheusden S., Suetens P., Marchal G., Sanderink G., Jacobs R.: Comparison between effective radiation dose of CBCT and MSCT scanners for dentomaxillofacial applications. *Eur J Radiol*, 2009, 71: 461-468.
5. Ludlow J.B., Ivanovic M.: Comparative dosimetry of dental CBCT devices and 64-slices CT for oral and maxillofacial radiology. *Surg Oral Med Oral Pathol Oral Radiol Endod*, 2008, 106: 106-114.
6. Miracle A.C., Mukherji S.K.: Conebeam CT of the head and neck, part 1: physical principles. *AJNR Am J Neuroradiol*, 2009, 30: 1088-1095.
7. Miracle A.C., Mukherji S.K.: Conebeam CT of the head and neck, part 2: clinical applications. *AJNR Am J Neuroradiol*, 2009, 30: 1285-1292.
8. De Vos W., Casselman J., Swennen G.R.J.: Cone-Beam computerized tomography (CBCT) imaging of the oral and maxillofacial region : A systematic review of the literature. *Int J Oral Maxillofacial Surg*, 2009, 38: 609-625.
9. Olszewski R., Cosnard G., Macq B., Mahy P., Reyhler H.: 3D CT-based cephalometric analysis: 3D cephalometric theoretical concept and software. *Neuroradiol*, 2006, 48: 853-862.
10. Swennen G.R., Schutyser F.: Three-dimensional cephalometry: spiral Multi-slice vs cone-beam computed tomography. *Am J Orthod Dentofacial Orthop*, 2006, 130: 410-416.
11. De Clerck H., Nguyen T, Koerich de Paula L., Cevitanes L.: Three-dimensional assessment of mandibular and glenoid fossa changes after bone-anchored Class III intermaxillary traction. *Am J Orthod Dentofacial Orthop*, 2012, 142: 25-31.
12. Albuquerque M.A., Gaia B.F., Cavalcanti M.G.P.: Comparison between multislice and cone-beam computerized tomography in the volumetric assessment of cleft palate. *Med Oral Pathol Oral Radiol Endod*, 2011, 112: 249-257.
13. Wörtche R., Hassfeld S., Lux C.J., Müssig E., Hensley F.W., Krempien R., Hofele C.: Clinical application of cone beam digital volume tomography in children with cleft lip and palate. *Dentomaxillofac Radiol*, 2006, 35: 88-94.
14. Zoumalan R.A., Lebowitz R.A., Wang E., Yung K, Babb J.S., Jacobs J.B.: Flat panel conebeam computed tomography of the sinuses. *Otolaryngology-Head and Neck Surgery*, 2009, 140: 841-844.
15. Maillet M., Bowles W.R., McClanahan S.I., John M.T., Ahmad M.: Cone-beam computed tomography evaluation of maxillary sinusitis. *J Endod*, 2011, 37: 753-757.
16. Pazera P., Bornstein M.M., Pazera A., Sendi P., Katsaros C.: Incidental maxillary sinus findings in orthodontic patients: a radiographic analysis using cone-beam computed tomography (CBCT). *Orthod Craniofac Res*, 2011, 14: 17-24.
17. Zain-Alabdeen E.H., Alsadhan R.I.: A comparative study of accuracy of detection of surface osseous changes in the temporomandibular joint using multidetector CT and cone beam CT. *Dentomaxillofacial Radiol*, 2012, 41: 185-191.
18. Barghan S., Tetradis S., Mallya S.M.: Application of cone beam computed tomography for assessment of the temporomandibular joints. *Australian Dental J*, 2012, 57: 109-118.
19. Librizzi Z.T., Tadinada A.S., Valiyaparambil J.V., Lurie A.G., Mallya S.M.: Cone-beam computed tomography to detect erosions of the temporomandibular joint: effect of field of view and voxel size on diagnostic efficacy and effective dose. *Am J Orthod Dentofacial Orthop*, 2011, 140: e25-e30.
20. Shintaku W.H., Venturin J.S., Noujeim M.: Applications of cone-beam computed tomography in fractures of the maxillofacial complex. *Dental Traumatology*, 2009, 25: 358-366.
21. Oluwasanmi A.F., Pinto A.L.: Management of nasal trauma – widespread misuse of radiographs. *Brit J Clin Governance*, 2000, 5: 83-85.
22. De Ceulaer J, Swennen G, Abeloos J, De Clercq C.: Presentation of a cone-beam CT scanning protocol for pre-prosthetic cranial bone grafting of the atrophic maxilla. *Int J Oral Maxillofac Surg*, 2012, 41 : 863-866.
23. Dahmani-Causse M., Marx M., Deguine O., Frayssse B., Lepage B, Escudé B.: Morphologic examination of the temporal bone by cone beam computed tomography: comparison with multislice helical computed tomography. *Eur Ann Otorhinolaryng Head and Neck diseases*, 2011, 128: 230-235.
24. Ruivo J., Mermuys K., Bacher K., Kuhweide R., Offeciers E., Casselman J.W.: Cone beam computed tomography, a low-dose imaging in the post-operative assessment of cochlear implantation. *Otol Neurotol*, 2009, 30: 299-303.
25. Trieger A., Schulze A., Schneider M., Mürbe D.: In vivo measurements of the insertion depth of cochlear implant arrays using flat-panel volume computed tomography. *Otol Neurotol*, 2010, 32: 152-157.
26. Penninger R.T., Tavassolie T.S., Carey J.P.: Cone-beam volumetric tomogra-

- phy for applications in the temporal bone. *Otol Neurotol*, 2011, 32: 453-460.
27. De Cock J., Mermuys K., Goubau J., Van Petegem S., Houthoofd B., Casselman J.W.: Cone-Beam computed tomography: a new low dose, high resolution technique of the wrist, presentation of three cases with technique. *Skeletal Radiol*, 2012, 41: 93-96.
28. Zbijewski W., De Jean P., Prakash P., Ding Y., Stayman J.W., Packard N., Senn R., Yang D., Yorkston J., Machado A, Carrino J.A., Siewerdsen J.H.: A dedicated cone-beam CT system for musculoskeletal extremities imaging: design, optimization, and initial performance characterization. *Am Assoc Phys Med*, 2011, 38: 4700-4713.
29. Smith E.J., Al-Sanawi H.A., Gammon B., St. John P.J., Pichora D.R., Ellis R.E.: Volume slicing of cone-beam computed tomography images for navigation of percutaneous scaphoid fixation. *Int J CARS*, 2012, 7: 433-444.
30. Wihlm R.R., Le Minor J.-M., Schmittbuhl M., Jeantroux J., Mac Mahon P., Veillon F., Dosch J.-C., Dietemann J.-L., Bierry G.: Cone-beam computed tomography arthrography: an innovative modality for the evaluation of wrist ligament and cartilage injuries. *Skeletal Radiol*, 2012, 41: 963-969.
31. Dreiseidler T, Ritter L, Rothamel D, Neugebauer J, Scheer M, Mischkowski R.A.: Salivary calculus diagnosis with 3-dimensional cone-beam computed tomography. *Oral Maxillofacial Radiol*, 2010, 110: 94-100.
32. Li B., Long X., Cheng Y., Wang S.: Cone beam CT sialography of stafne bone cavity. *Dentomaxillofac Radiol*, 2011, 40: 519-523.
33. Yoshihara M., Terajima M., Yanagita N., Hyakutake H., Kanomi R., Kitahara T., Takahashi I.: Three-dimensional analysis of the pharyngeal airway morphology in growing Japanese girls with and without cleft lip and palate. *Am J Orthod Dentofacial Orthop*, 2012, 141: S92-101.
34. El A.S., El H., Palomo J.M., Baur D.A.: A 3-dimensional airway analysis of an obstructive sleep apnea surgical correction with cone beam computed tomography. *J Oral Maxillofac Surg*, 2011, 69: 2424-2436.
35. Park S.B., Kim Y.I. Son W.S., Hwang D.S., Cho B.H.: Cone-beam computed tomography evaluation of short- and long-term airway change and stability after orthognatic surgery in patients with Class III skeletal deformities: bimaxillary surgery and mandibular setback surgery. *Int J Oral Maxillofac Surg*, 2012, 41: 87-93.
-